# FLARES ON THE SUN AND OTHER STARS

*Bernhard Haisch and Keith T. Strong*

Solar and Astrophysics Laboratory, Lockheed, Palo Alto, California

*Marcello Rodonò*

Institute of Astronomy, Catania University and Astrophysical Observatory, Catania, Italy

KEY WORDS:   X rays, variability, dMe stars, RS CVn stars

## 1.  INTRODUCTION

### 1.1   *The Practical Importance of Flare Research*

Solar flares have been known to cause widespread power outages and communication disruptions. They pose radiation hazards to instruments and reduce low-orbit-spacecraft lifetimes. (Ironically the *Solar Maximum Mission* (*SMM*) flare research satellite reentered early owing in part to flaring!) Flares are interesting to astrophysicists because they show extreme conditions of temperature ($T \approx 10^7$–$10^8$ K), density, and plasma motions. Flare activity in the current solar cycle (22) was predicted to peak in 1991, but actually peaked in July 1989 at an unexpectedly high level, a sobering reflection on our present understanding.

The March 10, 1989 X-flare produced a geomagnetic storm two days later that blacked out the Hydro-Quebec power system. Transformers failed, hundreds of relays and protective systems malfunctioned and voltage and power fluctuations were widespread in North America. Power networks now extend over such distances that extreme differences in ground potential arise, inducing strong currents (Kappenman & Albertson 1990).

275

Dosimeters registered alerts on high-flying Concordes during the October 1989 proton event. On long flights in the auroral zones (e.g. California to Europe) dosage of radiation equivalent to a chest X-ray can occur. Flares certainly pose a potentially lethal hazard to space travelers. The ability to understand, monitor, and predict solar activity must become a priority in the manned space program. Unfortunately, the only flare-research spacecraft programs actively underway are the Japanese *Solar-A* and Russian *Coronas*, scheduled for launch in 1991 and 1992, well after the cycle 22 maximum.

## 1.2  *The Astrophysical Importance of Flare Research*

Flares are important to astrophysics because they originate in out-of-equilibrium magnetic field–plasma interactions rather than in gravitational, thermonuclear, or radiative processes in near equilibrium. Flare stars constitute about 10% of the stars in the Galaxy. The time-integrated flare energy in the most active star may reach a few percent of $L_{bol}$. Very fast dMe flares may last only 2–3 s (Gershberg 1989). RS CVn flares may attain $10^{31}$ ergs s$^{-1}$. It has been proposed that cosmic rays originate in stellar flares (Meyer 1985a,b, Montmerle 1984).

The Sun is an invaluable proving ground to test predictions of flare theories and to develop analytical techniques for future stellar application. In turn, extreme flare star conditions push the limits of models. After a long lull we are again able to observe stellar flares via *ROSAT*, to be followed by *BBXRT, Spectrum-X, XTE, Astro-D*, and *AXAF*. With new instrumentation such as the E.S.O. New Technology Telescope (NTT) and the Hubble Space Telescope (HST), new observing techniques and diagnostics are opening up stellar flare physics once assumed to be beyond spatially unresolved observations.

## 1.3  *Flare Definition*

We define a flare as a catastrophic release of magnetic energy leading to particle acceleration and electromagnetic radiation, bearing in mind that the magnetic energy release and conversion has never been directly observed. Because flarelike physical processes occur in diverse astrophysically interesting regimes, the field of solar and stellar flares can serve as an astrophysical touchstone. For example, Aly & Kuijpers (1990) proposed that magnetic interactions between an accretion disk and a neutron star may result in periodic flares and Sturrock & Stern (1980) considered the possibility of galactic flares heating the galactic corona. Flaring may occur in many kinds of magnetospheres, in galactic nuclei and quasars, perhaps even in intergalactic regions—anywhere large scale dynamos may be operative (e.g. Belvedere et al 1989).

## 1.4  *Major Literature*

The pre-X-ray era text on flares was *Solar Flares* by Smith & Smith (1963). The books, *Solar Flares* by Svestka (1976) and *Solar Flares: A Monograph from Skylab Solar Workshop II* by Sturrock (1980) brought the topic into the modern era on the solar side, while the 1982 Catania Proceedings of IAU Colloquium No. 71, *Activity in Red Dwarf Stars* by Byrne and Rodonò (1983) brought the stellar side into the space age. In *Solar Flare Prediction*, Sawyer et al (1986) discussed the techniques of flare forecasting. A comprehensive textbook that includes flare physics is *Solar Magnetohydrodynamics* by Priest (1982). The textbook *The Physics of Solar Flares* by Tandberg-Hanssen & Emslie (1988) and the conference proceedings on *Solar and Stellar Flares* by Haisch & Rodonò (1989a,b) together give a current overview.

## 1.5  *Topics Not Covered*

For discussion of flare classification, we defer to the review of Bai & Sturrock (1989). We concentrate on observations that show the solar-stellar connection or point to probable future stellar observations. We do not address $\gamma$-ray and neutron production for which Ramaty & Murphy (1987) and Kocharov (1987) and references therein are recommended nor do we discuss in situ measurements of charged particles (see Dröge et al 1989, Moses et al 1989, Perez-Peraza 1986).

The development of hydrodynamic loop models has become a veritable cottage industry (from PCs to Crays). These solve the continuity, momentum, and energy equations for a one-dimensional flow by calculating the response to a given time-dependent heating function. Although developed for the Sun, they are being applied to stellar observations [see the Reale et al (1988) reanalysis of the 1980 Prox Cen flare and the simplified analysis model of Fisher & Hawley (1990)]. For overviews, see Emslie (1989) and Antonucci (1989). Lastly, the details of magnetic field reconnection, charged-particle acceleration, generation of Langmuir waves, etc also lie beyond the scope of this review (see Holman 1985, Heyvaerts 1981, McClements 1987, McClements 1989, LaRosa 1990).

## 2.  HISTORY OF SOLAR AND STELLAR FLARE OBSERVATIONS

### 2.1  *Solar Observations and Concepts*

Solar flares were discovered independently at 1118 GMT on September 1, 1859, by two English amateur astronomers, R. Hodgson (a brewery manager with a private observatory) and Richard C. Carrington (see Haisch

1989a). Engaged in sunspot projection sketching, they saw two crescent-shaped patches break out, brighten (<60 s), move a distance about twice their lengths, then fade away as two dots, all within 5 minutes. Both gave brief reports at a November 1859 Royal Astronomical Society meeting (Carrington 1860, Hodgson 1860, see Figure 1), Carrington commenting that "the magnetic instruments at Kew were simultaneously disturbed to a great extent . . . 4 hours after midnight there commenced a great magnetic storm." However the report adds, "While contemporary occurrence may

*Description of a Singular Appearance seen in the Sun on September 1, 1859. By R. C. Carrington, Esq.*

While engaged in the forenoon of Thursday, Sept. 1, in taking my customary observation of the forms and positions of the solar spots, an appearance was witnessed which I believe to be exceedingly rare. The image of the sun's disk was, as usual with me, projected on to a plate of glass coated with distemper of a pale straw colour, and at a distance and under a power which presented a picture of about 11 inches diameter. I had secured diagrams of all the groups and detached spots, and was engaged at the time in counting from a chronometer and recording the contacts of the spots with the cross-wires used in the observation, when within the area of the great north group (the size of which had previously excited general remark), two patches of intensely bright and white light broke out, in the positions indicated in the appended diagram by the letters A and B, and of the forms of the spaces left white.   My
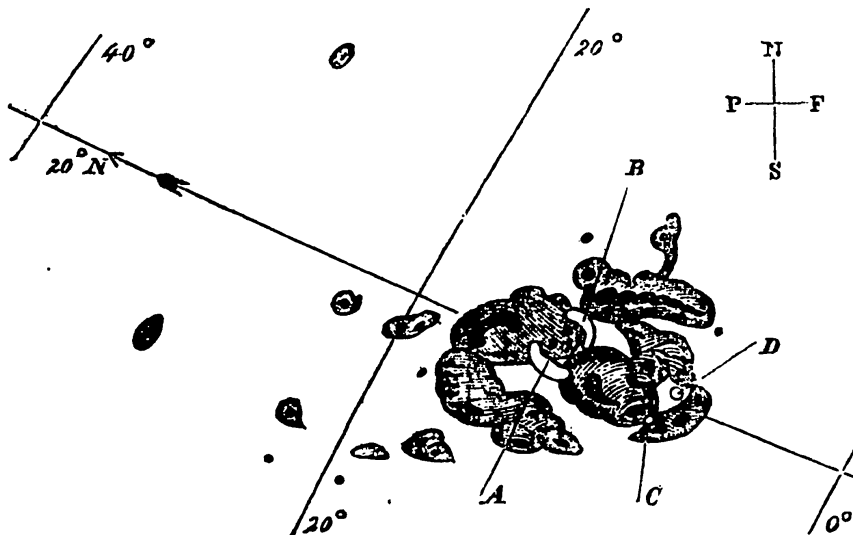


first impression was that by some chance a ray of light had penetrated a hole in the screen attached to the object-glass, by

*Figure 1* The article in an early 1860 issue of *Monthly Notices* announcing the discovery of a flare (called merely a "singular appearance") on the Sun.

deserve noting, he would not have it supposed that he even leans toward hastily connecting them. 'One swallow does not a summer make'." Lord Kelvin (William Thomson) later "proved" that the Sun could not possibly affect Earth in such a way, and this view prevailed (Sturrock 1987). For a discussion of 42 flare-related discoveries, see Hudson (1987).

Prior to the space era, virtually all flare observations involved photography in chromospheric lines: commonly Hα at 6563 Å, other Balmer lines, He I D3, Ca II H and K, Mg I b, and Na D. A major discovery was that flares occur along the magnetic neutral line (Severny 1958). The photospheric magnetic fields change little during a flare, while chromospheric fibril alignments do change, indicating a change in the magnetic potential energy higher up. Innovative solar cinematography with birefringent filters was developed by Moreton & Ramsey (1960) at the Lockheed Solar Observatory (Athay & Moreton 1961) and continues to be a major tool (Zirin 1988).

The dominant role of magnetic fields in the structure of the solar corona was established in the late 1960s by broad-band SXR telescopes (flown on rockets) that provided high resolution images (van Speybroek, Krieger & Vaiana 1970, Vaiana et al 1973). Magnetic fields are primarily generated by currents below the surface, constituting a potential field from which energy cannot be extracted. Currents in the corona produce a nonpotential component, which can be an energy source. Since Lorentz forces cannot be successfully opposed by gas pressure gradients above the chromosphere, only currents that are parallel to the potential field (and add a nonpotential twist) can flow. Such upflowing currents are determinable from surface vector magnetograms (Hagyard et al 1981). The goal is to measure the magnetic energy change with enough precision to equate this to the flare output.

The Orbiting Solar Observatory series (1962–1978) and the three *Skylab* missions (Orrall 1981) in 1973–1974 further opened up the UV and X-ray window, and demonstrated that the primary flare was not in the chromosphere. *SMM* ("Solar Max" to the media) was in operation in 1980, partially inoperative for three years, and back on the air following astronaut repair in April 1984 until reentry in December 1989. The Japanese *Hinotori* solar research satellite carried out hard X-ray (HXR) observations from February 1981 to October 1982 (see Tanaka 1983).

As to theory, Giovanelli (1948) developed a concept involving electric fields resulting from changes in adjacent sunspot magnetic fields. Later, Gold & Hoyle (1960) developed a theory that still concentrated on the chromospheric flare but included many of the modern essentials and can be termed a loop coalescence model (Sakai 1990). Other important work in the 1940s and 1950s was done by Cowling, Piddington, Dungey, Spitzer, Unsöld, Roberts, Billings, Sweet, and others (see Smith & Smith 1963).

## 2.2 *Stellar Observations*

On September 25, 1948, a spectrogram of the dMe dwarf star L726-8 by Joy & Humason (1949) revealed both line emission and continuum enhancement amounting to a change of about one magnitude. Thus began a long period of flare studies directed toward photometry of dKe/dMe UV Ceti-type stars in the *U*- and *B*-bands. Studies concentrated on flare occurrence versus energy for different stars, measurement of flare colors and their temporal evolution, and recombination modeling of the optical radiation (Gershberg 1967, Moffett 1974, Cristaldi & Rodonò 1975, Kunkel 1975).

Stellar radio flares also turned out to be unexpectedly bright (UV Ceti and EV Lac by Lovell et al 1963 and Lovell et al 1964, V371 Ori by Slee et al 1964), but studies of this type languished until the mid 1970s when interferometric techniques (Gibson 1983) and the VLA came into use (Kundu & Lang 1985, Rodonò 1986a).

When the EUV/X-ray window finally opened on the stellar side to reveal the high energy flare (Heise et al 1975, Haisch et al 1977), solar and stellar studies at last emerged from their mutual isolation and began the current trend of cross-fertilization.

## 3. CLASSES OF FLARE STARS

G dwarfs should flare if the Sun is typical, but, because of low optical contrast of a flare against the disk integrated flux, researchers could not directly observe such flares until *Exosat* measured a large flare ($L_x = 10^{30}$ ergs s$^{-1}$) on the active, rapidly rotating G0 V star $\pi^1$ U Ma (Landini et al 1986). Other types of stars are likely to flare, but determining the true source is problematic. For example, although there is an *Exosat* observation of a flare on Castor AB—two A-type stars ($<6''$ separation) well away ($70''$) from the flare star binary Castor C (YY Gem)—both A and B are themselves single-lined spectroscopic binaries (Pallavicini et al 1990a). The archetypal flare star UV Ceti is also a binary. (See Geyer et al 1988 for a recent determination of stellar parameters and orbit.)

Pettersen (1989) has reviewed flaring activity across the HR diagram. Schaeffer (1989) has presented a compilation of flashes ranging up to 7 mag on several dozen stars. Herein we concern ourselves with the Sun, the dwarf K and M stars, the pre-main sequence T Tauri and FU Orionis stars, and RS CVn systems.

Programs have recently begun seeking to correlate flare activity with age by comparing field flare stars with cluster flare stars (Tsvetkov & Tsvetkova 1990, Aniol et al 1990). The most distant catalogued field dMe

flare star is at 21 pc (Pettersen 1976), while the Hyades cluster is twice as distant (42 pc), the Pleiades are at 127 pc, and the Orion associations are at approximately 400 pc. These low-mass stars evolve slowly: The approximate main-sequence lifetimes are $40 \times 10^9$ years for a dK5, $70 \times 10^9$ years for a dM0, and $270 \times 10^9$ years for a dM5. Several hundred flaring objects have been catalogued in Orion and the Pleiades. Studies by Mirzoyan et al (1988) indicate that field and cluster/association flare stars do represent the same class. They also estimate that the Galaxy contains $4.2 \times 10^9$ UV Ceti-type flare stars, which probably originated—as did most stars—in clusters and associations that have since broken up (see also Szécsényi-Nagy 1990).

Pre-main-sequence stars show high levels of magnetic activity (Feigelson et al 1990, Montmerle 1990) and strong flares. FU Orionis stars may be a phase between T Tauri and post-T Tauri, the entire sequence corresponding to disappearance of circumstellar material. X-ray and radio flares in stars in the $\rho$ Oph and other dark clouds show flaring as energetic as that in the RS CVn systems. Some of this variability may result from changes in the obscuration and mass infall, but magnetic interactions between the disk and the star may also occur (Kuijpers 1989).

Radio mapping of the Pleiades shows no evidence for the giant radio flares reported in star-forming regions (Bastian et al 1988), implying that whatever the cause, the mechanism lasts <few $\times 10^7$ years.

An X-ray flare was observed on van Biesbrock 8, which is one of the faintest known M dwarfs: a dM7e with $L \approx 5 \times 10^{-4} L_\odot$ assumed to be fully convective (Tagliaferri et al 1990). This observation is important vis-a-vis the issue of where the dynamo is situated.

## 4.   THE FLARE IN VARIOUS SPECTRAL REGIONS

Flares produce emissions from $\gamma$ rays to the radio, each part revealing a different aspect, which is why simultaneous data taken at many wavelengths are important (see Strong et al 1984). For this reason, *SMM* covered from 140 MeV to the visible and many ground-based simultaneous observations were made at radio (VLA, Clark Lake, Meudon, Owens Valley) and optical (SOON network, MSFC, Sac Peak, BBSO) wavelengths. A multiwavelength approach was the theme of the *Solar and Stellar Flares* IAU Colloquium (Haisch & Rodonò 1989a,b). Considerable information can be derived from the timing and spectral behavior of unresolved, full-Sun observations. For example, the millisecond variations measured at radio and HXR wavelengths are probably signatures of the primary flare energy release. Such techniques are being used to study stars.

## 4.1   *The Venerable Hα Flare*

Solar flares have long been classified by an Hα scheme: area importance as *S* (subflare), 1, 2, 3, or 4; brightness as f(aint), n(ormal) or b(rilliant). A major flare may show disk-integrated Hα going from about 80% central depth absorption to emission at twice the continuum with 2–3 times the absorption width (L. W. Acton, private communication), but since the area involved is less than 0.01% of the disk, the integrated line will change <0.1%.

On dMe stars, Hα almost invariably appears in emission with quiescent equivalent width of about 2 Å. During flares, this may increase by >10 with line broadening and red or blue asymmetries indicating random motions of 100 km s$^{-1}$ and mass flows at speeds up to 1000 km s$^{-1}$ (cf Rodonò 1986b). A characteristic of Hα is the central reversal, with half width of about 1 Å, apparent in spectra with resolution <0.1 Å. Worden & Peterson (1976) and Worden et al (1981) interpret the reversal in terms of optically thick emitting regions in the Hα emission-line core similar to solar plages, spicules, and prominences. This feature is highly variable (Bopp 1974), suggesting transient changes in the physical conditions of the emitting plasma.

There is a correlation between Hα flare importance and total Hα energy from which an X-ray vs Hα relation is found (Thomas & Teske 1971, Mayfield & Lawrence 1985). This correlation is essentially the same for the dMe stars as for the Sun, although wide variations occur for individual flares (Butler et al 1988, Haisch 1989b).

## 4.2   *Solar White Light Flares and Stellar Optical Flares*

In disk-integrated optical light, the Sun is not a flare star. The Active Cavity Radiometer Irradiance Monitor (ACRIM) on *SMM* failed to detect even major flares because of limited size and low photospheric contrast (~20%); one sees at most a 0.01% irradiance change. Flare stars are different because the ratio of flare to nonflare emission can be much higher and the low $T_{eff}$ of dwarf K and M stars increases the *U* and *B* contrast.

White light flares (WLFs) apparently become visible whenever the X-ray flare exceeds a certain threshold. The WLF also apparently represents the major portion of the radiative output (Neidig et al 1989). The most energetic WLF attained $L = 2 \times 10^{29}$ ergs s$^{-1}$ and $E > 3 \times 10^{31}$ ergs. WLFs have a flat intensity spectrum from 6000 to 4000 Å, but increase markedly (factor of 2–3) at shorter wavelengths (Balmer jump). Estimates suggest that 90% of the emission is continuum and the rest is in the form of lines. See Mauas (1990), Donati-Falchi et al (1985), and Hiei (1982) for discussion of the WLF spectrum; recent reviews include Hiei (1987) and Neidig (1989).

Stellar optical flares probably involve larger areas and perhaps brighter surface fluxes than WLFs (e.g. Falchi et al 1990). The 2-mag $U$-band flare reported by Rodonò et al (1989) on AD Leo corresponds to $L_U = 8 \times 10^{29}$ ergs s$^{-1}$; the 0.22 magnitude $U$-band flare reported by deJager et al (1986) on BY Dra corresponds to $L_U = 1.3 \times 10^{30}$ ergs s$^{-1}$. At a given rate of occurrence, optical flares on dMe stars are typically 10–1000 times as energetic as solar flares (see Figure 2 in Shakhovskaya 1989).

## 4.3  Soft X-Ray Flares

The disk-integrated solar SXR emission has been monitored since 1976 by the *Geostationary Operational Environmental Satellites* (*GOES*) (Donnelly et al 1977, Thomas et al 1985). The ratio of the two available bands indicates the peak temperature of the flare plasma. A flare scheme has been developed by NOAA on the basis of the peak flux in the 1–8 Å band; a classification of B, C, M, or X is assigned, each corresponding to a factor of ten change (Sawyer et al 1986) (thus an X1 flare corresponds to $f_{1-8} = 10^{-1}$ ergs cm$^{-2}$ s$^{-1}$; an X2 flare has twice the flux, etc). The most intense flare is estimated to have been on the order of X20, which would correspond to $L_x \approx 6 \times 10^{27}$ ergs s$^{-1}$ total power, almost as intense as the 1980 *Einstein* Prox Cen flare (Haisch et al 1983). The total energy involved in that 13-h solar event was $E \sim 2.5 \times 10^{31}$ ergs (J. Saba, private communication).

RS CVn systems have very intense SXR flares. (The "giant X-ray flare" in the Hyades observed by Stern et al 1983, with $L_x > 10^{31}$ ergs s$^{-1}$, was probably an RS CVn.) X-ray flares were observed on Algol by *Exosat* (van den Oord & Mewe 1989) and *Ginga* (Stern et al 1990a); and on $\sigma^2$ Cor Bor by *Einstein* (Agrawal et al 1986), *Exosat* (van den Oord et al 1988), and *Ginga* (Stern et al 1990b). The Algol flare observed by *Ginga* on January 13–14, 1989, lasted longer than 12 hours, had a peak $L_x \approx 10^{31}$ ergs s$^{-1}$, and a maximum temperature $T \approx 69$ MK. Although it was shorter in duration (4 h), the peak $L_x \approx 1.6 \times 10^{31}$ ergs s$^{-1}$ and $T \approx 78$ MK observed on Algol by *Exosat* on August 18, 1983, are practically the same as those for the *Ginga* flare. The peak luminosity of the *Einstein* flare on $\sigma^2$ Cor Bor is comparable: $L_x \approx 6 \times 10^{30}$ ergs s$^{-1}$.

## 4.4  Ultraviolet Continuum

The solar flare UV continuum—arising at the temperature minimum—appears shortward of the Si I edge at 1683 Å. Cheng & Kjeldseth Moe (1978) compared the (1400–1960 Å) EUV continuum with the (8–20 Å) SXR for the September 5, 1973, *Skylab* flare and found more energy in the EUV.

Strong ultraviolet continua have been detected by *IUE* in a few stellar

flares. Butler et al (1981) first measured this phenomenon on Gl 867A (FK Aqr). Byrne & McKay (1990) observed these continua during a large flare on the rapidly rotating dM2.5e star Gl 890. Mathioudakis & Doyle (1990) report on a UV enhancement in Gl 644AB. These spectra appear to be free-free emission ($T \sim$ 14,000–50,000 K), with $f_{cont}/f_{CIV} \approx$ 13–39.

Very few UV solar flare observations exist. Bromage et al (1986) compared the June 15, 1973, *Skylab* flare to an *IUE* flare [observed with the short-wavelength spectrograph primary camera (SWP)] on AT Mic; the total emitted power (ergs s$^{-1}$) in the AT Mic UV lines is $\sim 10^4$–$10^5$ times the power in that solar flare. Similarly, the UV continuum is $10^3$–$10^5$ times greater than that of a solar flare.

## 4.5    Radio Flares

The concept of an intensity vs frequency radiospectrogram or *dynamic spectrum* was introduced by Wild (1950a,b). These are categorized as bursts of Type I, II, III, IV, or V and are typically observed in the 50–300 MHz range. Type III bursts occur during the impulsive phase of a flare and appear to be a consequence of electron beams because of an apparent one-to-one correspondence with HXR bursts (Reames 1990, Raoult et al 1985). A discussion of the relation of radio bursts to particle acceleration and mass ejection may be found in Melrose & Dulk (1987).

Stellar radio flares are up to $10^5$ times as luminous as solar. The first dynamic spectrum was obtained with the VLA on the RS CVn-type UX Ari at five frequencies (Hjellming & Gibson 1980). During the decay phase of a flare event on another RS CVn-type system (AR Lac) observed with the VLA at three frequencies, an inversion of the flare spectral index was found for the first time (Rodonò et al 1984). Better defined dynamic spectra of stellar flares were obtained by Bastian & Bookbinder (1987), who observed a 50-MHz band (in 15 channels) at 1415 MHz for the star UV Ceti. In addition to incoherent gyrosynchroton emission, they discovered highly polarized ($T_b > 10^{11}$ K) bursts interpreted as coherent emission. Even more intense ($T_b \approx 10^{16}$ K) emission was found on AD Leo and YZ CMi (Bastian et al 1990). Such coherent emission could be produced by either plasma radiation or a cyclotron maser instability. Rise times of $\leq 20$ ms and durations of $\leq 50$ ms characterized some of the radio spikes.

## 4.6    Hard X Rays

Although a great deal of largely unobserved activity probably precedes HXR bursts (see below), they serve to mark the flare onset. The higher the energy, the spikier is the light curve (shown in Figure 2, along with the WLF/HXR correlation). A HXR classification scheme has been based on *Hinotori* observations (Tsuneta 1983, Tanaka 1987) consisting of Type A
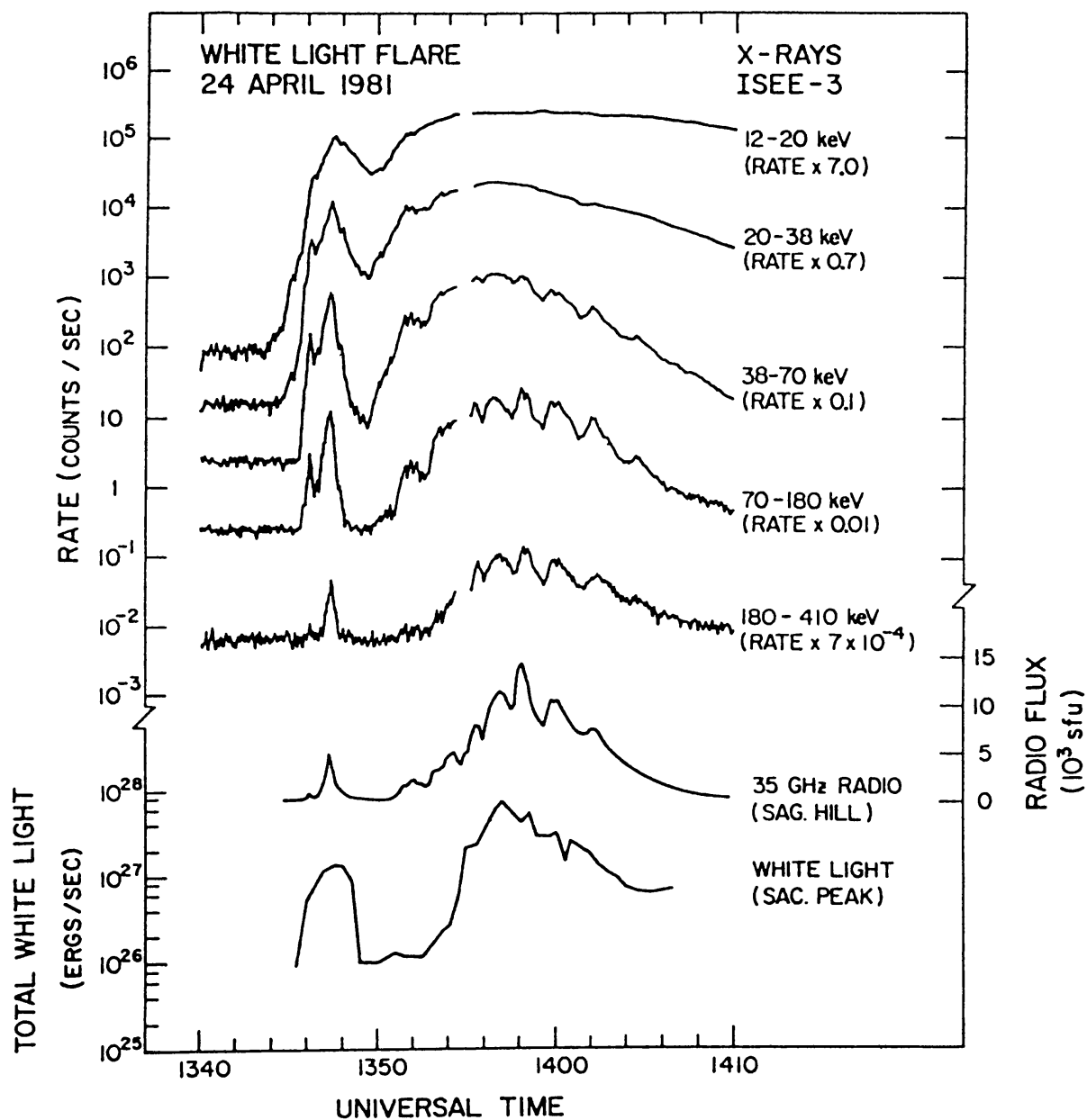
*Figure 2* Light curves for the White Light Flare of April 24, 1981, showing the relationship of hard X rays, white light, and radio time profiles (from Kane et al 1985).

(Hot Thermal Flare), Type B (Impulsive Flare), and Type C (Gradual-Hard Flare). Pearson et al (1989) have examined the HXR characteristics of 2500 flares.

Stellar hard X rays are presently unobservable. The *Exosat* 7–10 keV detections [from the medium energy experiment (ME), e.g. Haisch et al 1987] are mostly extensions of the SXR light curve.

# 5.   THE PHYSICS OF FLARES

Several flare scenarios have been developed. The difficulty is to explain the trigger mechanism, the timing of the various flare components (radiation, ejecta, and accelerated particles; see Katsova & Livshits 1987), the changing spectral distribution over a huge range of wavelengths as the flare evolves, and cooling mechanisms. No model has been able to describe all aspects, nor do we have a reliable and comprehensive energy budget; nevertheless substantial progress on individual mechanisms has been made. A reference model is useful as a guide to define questions, suggest observations, and assist our conceptualization. We consider the flare model of Martens & Kuin (1989).

## 5.1   *The Martens and Kuin Two-Ribbon Flare Model*

Kiepenheuer (1964) first proposed that two-ribbon flares and filament eruptions are different manifestations of the same phenomenon, and some researchers have concluded that all flares are driven by eruptions (Hirayama 1974, Moore 1988, Martin 1990, Zirin 1988). A concept for the magnetic configuration and the location of the major physical phenomena was first presented by Carmichael (1964).

Figure 3 [from Martens & Kuin (1989)] reviews most aspects of this scenario; earlier versions of this figure have been put forward by Hirayama (1974), Van Tend & Kuperus (1978), Pneuman (1980), Cliver (1983), Hagyard et al (1984), Kaastra (1985), and Dennis (1985). Shown is a cross section perpendicular to the photospheric polarity inversion line. The lines with arrows are the **B** projections. Owing to the presence of a magnetic field component perpendicular to the figure, the closed field lines represent a helical flux tube that connects back to the photosphere at the endpoints of the filament, so, contrary to appearance, there are no open field lines. The existence of closed (in projection) field lines implies the presence of a net current in the direction of the axis of the filament (the center of the tube). This current is the ultimate source of free magnetic energy that fuels the flare. Cool matter—observed in Hα as the filament—is supported in the trough of the field lines.

Prior to the two-ribbon flare, the filament erupts. The eruption may be caused by: (*a*) "loss of equilibrium" as the filament current surpasses a certain threshold (Van Tend & Kuperus 1978, Low 1977; but see the recent analysis by Forbes 1990 and arguments against this concept by Klimchuk & Sturrock 1989); (*b*) a slow withering away of the overlying arcade of coronal loops by gentle preflare reconnection in the current sheet below the filament (Sturrock et al 1984), until, again, loss of equilibrium sets in; or (*c*) a different scenario—supported by the numerical MHD model of
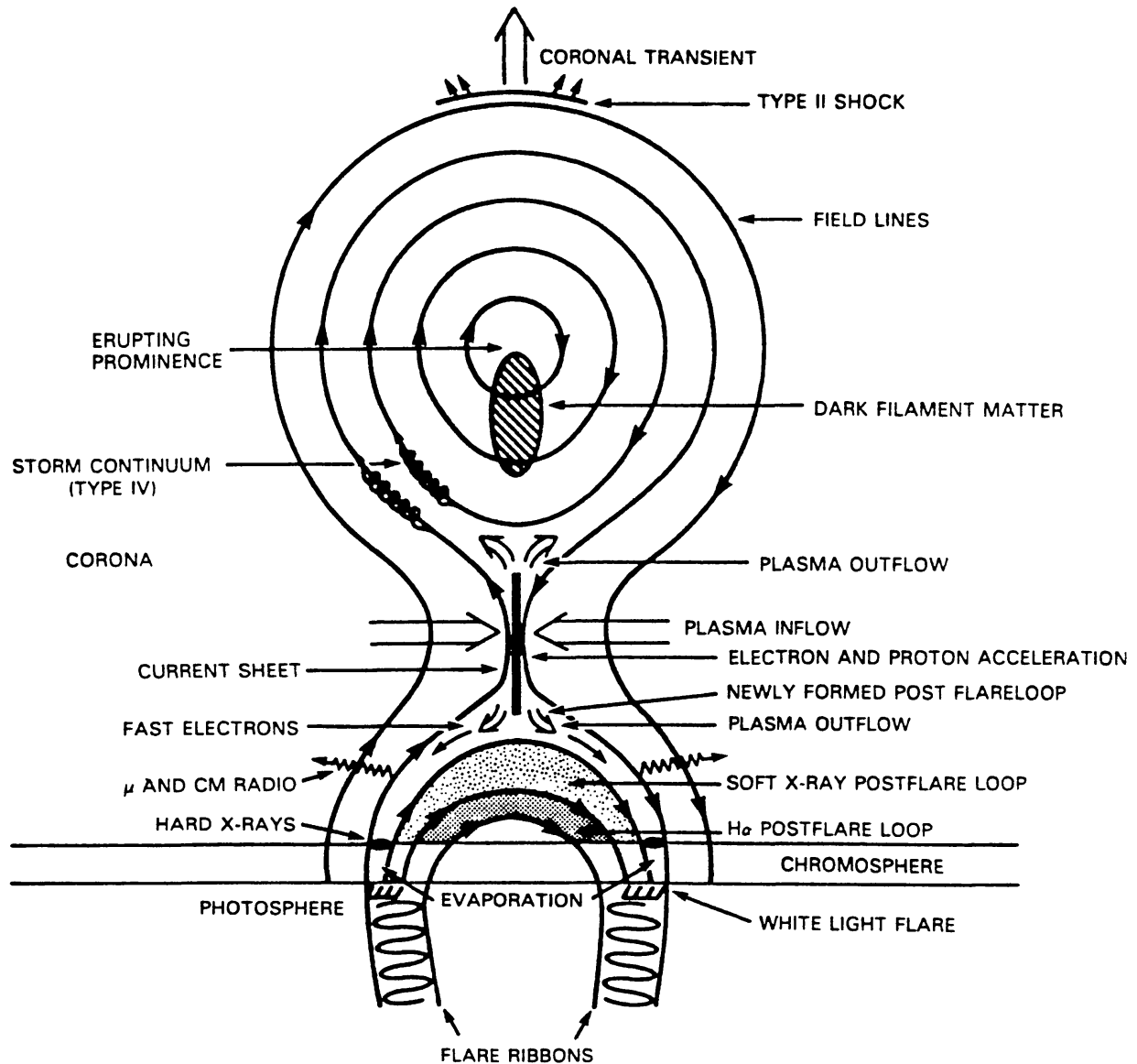
*Figure 3*   The global structure of the Martens & Kuin two-ribbon flare model showing the location of the major observed energy conversion processes, viewed in a cross section along the neutral line (from Martens & Kuin 1990).

van Ballegooijen & Martens (1989)—in which the equilibrium height of the filament increases at an accelerating rate in response to photospheric flux cancellation at a constant rate; in this scenario, loss of equilibrium never occurs, but an eruption is still initiated. Shibata et al (1989) have done a 2-D MHD simulation of emerging flux; see also the current loop model of Chen (1989).

As the filament erupts, the reconnection rate in the current sheet in its wake is strongly enhanced because of field gradients created by stretching

of the whole field configuration. The energy released by the reconnection in this sheet fuels most of the two-ribbon flare phenomena. Much of the free magnetic energy is converted into kinetic energy of protons and electrons by acceleration in the sheet's **E** field. These accelerated particles precipitate into the chromosphere along the field lines and generate both hard X rays at the impact site and Hα ribbons. The energy deposited by the particle beams further drives chromospheric evaporation (ablation) that fills the postflare loops with hot material. Fast electrons also emit microwave gyrosynchrotron radiation as they spiral downward.

The arcades of magnetic loops formed at the reconnection site emit in soft X rays after being filled with evaporated material. As the flare progresses, reconnection produces higher and higher arcades of loops, and the Hα ribbons at the footpoints of these arcades move away from the photospheric neutral line. After formation, an arcade of loops is disconnected from its energy source, and these postflare loops cool down gradually, emitting initially in soft X rays, then in UV, and finally in Hα.

Higher up, fast electrons escaping upward from the current sheet cause Type IV gyrosynchrotron emission. In this scenario, a coronal mass ejection (CME) is caused by the density, and, hence, emission enhancement where the filament flux tube pushes against the overlying coronal arcade. Note that the observed filament lies much lower, in the bottom half of the flux tube. The Type II radio emission is thought to be generated at the site of the transient by the push of the filament tube.

Martens & Kuin also argue that the filament eruption causes the CME, and not vice versa, despite the observation that the CME eruption velocity is greater than that of the filament. Their simulations indicate that the filament flux tube expands while it erupts, which might explain this observation within the scenario presented here.

The recognition that flux cancellation may be "a necessary, evolutionary precondition for flares" (Livi et al 1989) and the association of flares with filament eruptions have led to the prominence model of Figure 4 (van Ballegooijen & Martens 1989). An initial potential field is sheared as a result of flow both parallel and perpendicular to the neutral line; reconnection forms loops *AD* and *CB*; loop *CB* submerges, and loop *AD* begins to interact with overlying sheared loops leading to a helical loop *EH*, which may contain the filament material.

## 5.2   *Coronal Mass Ejections*

CMEs are very large-scale ($\sim R_\odot$) erupting looplike features visible in white light coronagraphs (see Chapter 8 of Zirin 1988). They occur at a rate of nearly one per day and involve substantial mass and energy: $10^{15}$–
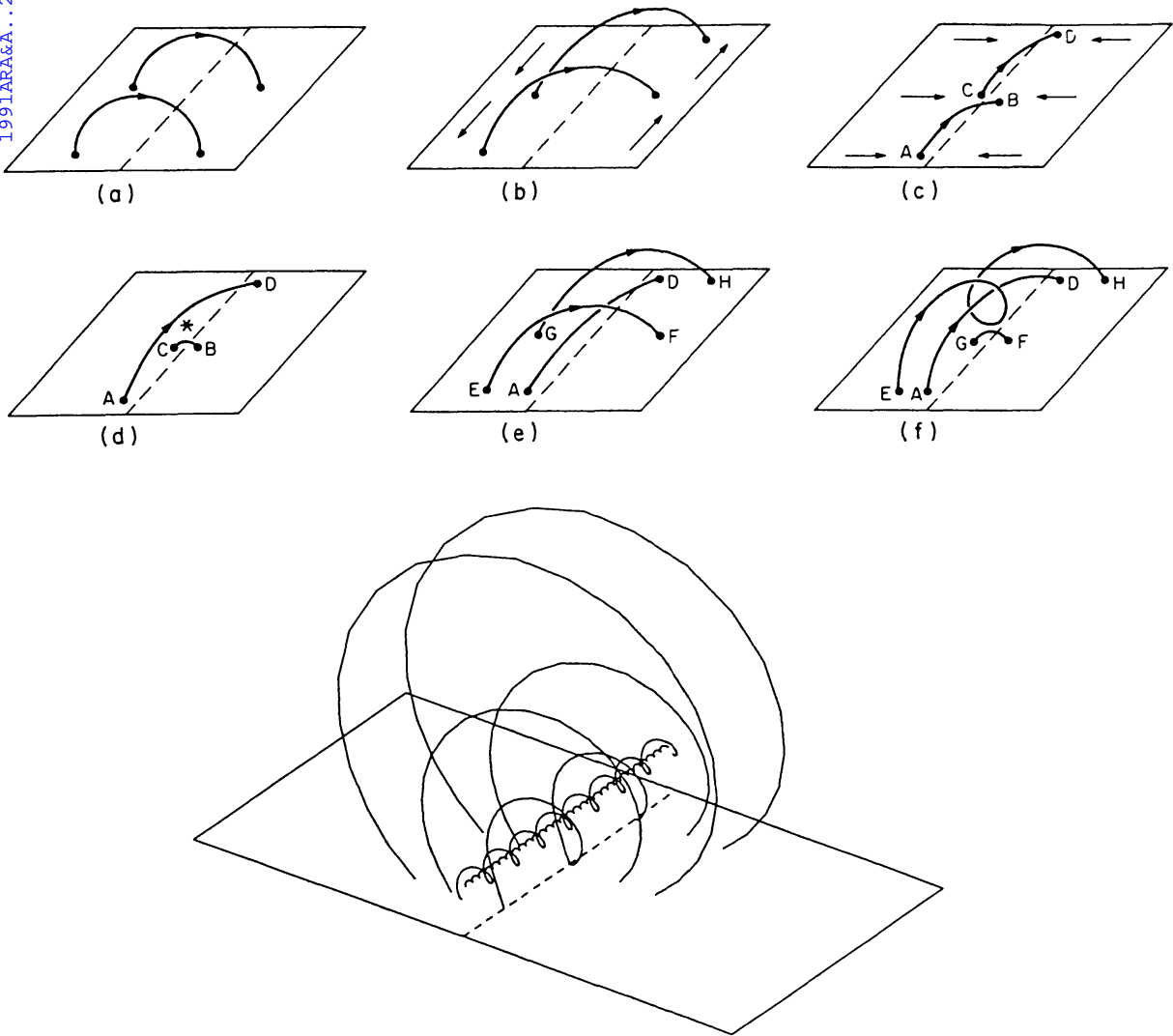
*Figure 4* (*Top*) Flux cancellation in shearing magnetic fields along the neutral line resulting in prominence formation. (*a*) Initial potential field; (*b*) sheared field resulting from component of flow parallel to neutral line; (*c*) component of flow toward neutral line increasing shear; (*d*) reconnection forms loops *AD* and *CB*; (*e*) loop *CB* submerged and loop *AD* beginning to interact with overlying sheared loops *EF* and *GH*; (*f*) helical loop *EH* formed while *GF* submerges. (*Bottom*) A larger-scale view of the overlying field (from van Ballegooijen & Martens 1989).

$10^{16}$ g and $10^{30}$–$10^{32}$ ergs. Because they are seen only after crossing the coronagraph occulting disk ($\sim 0.2R_{\odot}$), both geometrical projection and acceleration profile assumptions are necessary to determine their origin.

CMEs are associated with flares and prominence eruptions (Munro et al 1979, Webb & Hundhausen 1987, Gopalswamy & Kundu 1987, Harrison & Sime 1989); at issue is which causes which. (Note that estimated CME energies often exceed that of the associated flare.) To address this

question systematically, a CME Onset Program was initiated in 1985 by using the Coronagraph/Polarimeter (C/P) and the X-ray Polychromator on *SMM*. On the basis of 16 data sets, Harrison et al (1990) found that CME launches precede major X-ray flares by tens of minutes, and that a majority of CMEs are associated with eruptive prominences. The picture they paint is the following: A weak SXR burst signals the onset of the rising of a large-scale magnetic structure; some tens of minutes later a region of magnetic complexity at one of the CME footpoints destabilizes because of stresses from the field line stretching above, and this destabilization results in particle acceleration, reconnection, and heating [i.e. a flare underneath and off to one side (footpoint) of the CME]. An erupting prominence may also occur underneath the rising CME, but it is unaffected by the flare activity below. The CME then continues to rise as a result of magnetic buoyancy of the disconnecting bubble following the "melon seed mechanism" model of Pneuman (1984). The frequent occurrence of preimpulsive microwave emission is evidence for such a model because this emission signals the presence of energetic electrons in the corona up to several minutes before the impulsive phase (Pick et al 1990).

Clearly CMEs, prominence eruptions, and flares are intimately related. As photospheric flow patterns push opposite-polarity loop footpoints together and as new emerging flux rises, cancellation leads to the formation of an X-type topology along the neutral line. Within this cavity, cool material may collect, forming a filament. Larger-scale overlying fields act like strings holding down the cavity, but, with the continuous appearance of new flux everywhere, cancellation cuts the strings and allows the X-type point to rise. At some point a current sheet forms, and the weakening of overlying fields gives rise to a CME, followed by prominence eruption and a flare. According to Parker (1989), magnetic shear of an arcade of parallel loops ("quonset hut") along a neutral line can increase the magnetic energy without bound; however at some point of critical shear the energy state will be lower if a reconfiguration extends the field lines radially to infinity. Such a transition from sheared arcade to radial open field pitches coronal gas outward, thereby creating a CME (see also Priest 1988).

### 5.3    *Flare Dynamics*

Mass motions and line broadenings in coronal plasma above active regions were discovered using SXR line spectroscopy with *SMM* (Acton et al 1981, Saba & Strong 1990). Observations of line shifts and profile changes during a flare are as important as absolute flux or line ratio determinations (Watanabe 1987). The random mass motions appear to decrease during the impulsive part of the flare from about 160 to $<60$ km s$^{-1}$; the blueshifted component is typically 300 km s$^{-1}$ in SXR lines. This blueshift is usually

taken as evidence of chromospheric evaporation, but this argument has pros and cons (see Doschek 1990). It is still unresolved whether the large nonthermal broadening of SXR lines at the onset of flares (Antonucci et al 1986) results from turbulence, Doppler broadening owing to random streams, or other factors.

A consistent picture of high velocity evaporation emerged during the April 24, 1984, X13 flare. Antonucci et al (1990) found three distinct episodes separated by $\sim 1$ min during the impulsive phase, in which blueshifted SXR lines indicate sudden upflows of about 700–800 km s$^{-1}$; these correspond to observed increases in H$\alpha$ area; moreover these streams rapidly decelerate. Their interpretation was that ". . . a new injection of chromospheric plasma occurs when a new set of loops is involved in the flare." They find flare upflow blueshifts of 500 km s$^{-1}$ in Ca XIX spectra and up to 800 km s$^{-1}$ in Fe XXV. Maximum evaporation coincides with the peak of the HXR burst.

A simple, basic flare model is as follows (Acton et al 1982). Electron beams from the corona stream into the lower atmosphere and, in the process of spiraling down the magnetic field lines, produce gyrosynchrotron microwave emission; then, upon being stopped by ions, emit HXR bremsstrahlung. Some of the energy also goes into heating chromospheric material to flare temperatures of 10–20 MK; this process of chromospheric evaporation fills the coronal loops with hot plasma as shown by the SXR emitting material with nonthermal broadenings of 100–200 km s$^{-1}$, and the aforementioned Doppler shifts (first seen by the *P78-1* SOLFLEX experiment, Feldman et al 1980; later observed extensively by the *SMM* BCS experiment, Antonucci et al 1982) in SXR lines occurs concurrently with the HXR bursts. The fact that the radiative cooling curve decreases with increasing temperature between $5 \times 10^5$ and $10^7$ K (McWhirter et al 1975, Raymond et al 1976) leads to the runaway increase to flare temperatures until conduction finally takes over.

Chromospheric heating/evaporation is supported by the momentum balance analysis of Zarro et al (1988) and Canfield et al (1990); they compared the upflows implied by Ca XIX blueshifts with simultaneous H$\alpha$ redshifts during five solar flares. These oppositely directed flows appeared during the impulsive HXR emission. Estimating densities and volumes, these authors arrived at an approximate balance between the two flows during four flares. Bentley et al (1986) observed individual transient blueshifted features in Ca XIX and Fe XXV coincident with HXR spikes that can be interpreted as discrete high velocity streams, also suggesting explosive evaporation.

Naturally, observations have produced worrisome and problematic exceptions. For example, recently, Cheng (1990) found in the *Skylab* data

what may be the only well-observed preflare and impulsive UV spectra of a flare (January 21, 1974). These show enhanced emission and large turbulent broadening before the appearance of impulsive hard X rays. Moreover, no blueshifted component appears in the 1354 Å Fe XXI line to indicate chromospheric evaporation. Thus this flare contradicts the simple flare scenario: Electron beams could not have been the exciting agents, and chromospheric evaporation does not appear to have been significant. Feldman (1990) in fact argues that the beam-driven evaporation model is not supported by observations from large, nonimpulsive flares.

## 5.4    White Light Flare Production

Najita & Orrall (1971) and Hudson (1972) proposed that WLFs could be explained by bombardment of the chromosphere/upper photosphere by downstreaming proton or electron beams. Increased hydrogen ionization would enhance the hydrogen recombination spectrum. On the other hand, the $H^-$ absorption should also increase, causing a transient decrease of the net radiation (dip), a possible mechanism for so-called negative stellar flaring. The analysis of data sets collected at Catania Observatory for several flare stars has shown that 5–15% of flares are preceded by dips; on the other hand about 40% show small flux increases (Cristaldi et al 1980, Grinin 1983).

Other mechanisms that could heat this region and produce a WLF include irradiation (EUV and SXR), dissipation of Alfvén waves, dissipation of fine-scale currents, and enhanced absorption of photospheric radiation via $H^-$ (Metcalf et al 1990). Aboudarham & Henoux (1987, 1989) have modeled the various competing effects of electron beams. They show that electrons of $E > 80\,\mathrm{keV}$ (assuming a $\delta = 4$ power law index) are energetic enough to penetrate into the low chromosphere and temperature minimum (TM) region and heat the atmosphere enough to result in white light emission. An electron beam flux of $10^{12}$ ergs cm$^{-2}$ s$^{-1}$ would heat the TM region by about 240 K, leading to a strong white light contrast.

Metcalf et al (1990) have combined HXRBS observations and measurements of two spectral lines forming in the TM region before and during a solar flare (February 3, 1986) to test the proposed WLF mechanisms. They argue against the electron-beam heating mechanism on the grounds that the spectral index is too soft ($\delta = 6$, i.e. steeper high energy falloff, hence softer) for the Aboudarham & Henoux mechanism and that the TM enhancement persists 4 min after the end of the HXR burst. Machado et al (1989) have investigated the effects of radiative backwarming in WLFs. Heating that raises the temperature to about $10^4$ K in deep chromospheric layers ($n_H > 10^{14}$ cm$^{-3}$) results in Paschen emission of sufficient optical

depth to show up against the photospheric background and at the same time radiatively heats the TM region ($n_H > 10^{16}$ cm$^{-3}$) by about 100 K, resulting in an even more dominant continuum component from H$^-$ emission. In this way, a net radiative input of $\geq 10^{10}$ ergs cm$^{-2}$ s$^{-1}$ can account for WLFs. They argue, however, that heating at this chromospheric level would require that amount of flux from $E > 170$ keV electron beams, thus requiring $10^{12}$–$10^{14}$ ergs cm$^{-2}$ s$^{-1}$ (depending on the electron energy spectrum) down to the 20-keV level. Such electron fluxes are considered impossibly large. On the other hand, a $2 \times 10^{10}$ ergs cm$^{-2}$ s$^{-1}$ beam of $E > 6$ MeV protons would work; these would manifest a 3–30 Å redshifted component in L$\alpha$.

## 5.5 Electron Beams and Proton Beams in Hard X-Ray Flares

There appear to be four mechanisms for HXR production: creation of a $T > 10^8$ K plasma, electron beams [see Li & Emslie (1990) for differences in signatures], proton beams, and, finally, equal amounts of protons and electrons in a neutral beam, originally proposed by Simnett & Strong (1984).

In the "thin-target" model, electrons interact with ions (and each other, but this is negligible; see Svestka 1976, p. 155) to produce bremsstrahlung, but most electrons escape before losing a significant fraction of their energy; this process would have to occur high up. In the "thick-target" bremsstrahlung model, the electrons lose essentially all their energy via collisions with ions; this process would take place at the loop footpoints or in dense coronal loops. In both cases, the observed photon spectrum is related to the energy distribution of accelerated electrons. If the photon spectrum of the hard X rays is observed to be a power law, $I(E) \propto E^{-\gamma}$, then in the thin-target regime the electron energy distribution must be $N(E) \propto E^{-(\gamma - 0.5)}$, whereas in the thick-target regime the same $I(E)$ would require $N(E) \propto E^{-(\gamma + 1.0)}$ (Hudson 1972). One cannot determine the production mechanism from observation of $I(E)$.

In HXR emission from loop footpoints, thick-target bremsstrahlung occurs. In some flares, in which a HXR source persists high in the corona, either mechanism is possible. If the column density is less than $\approx 10^{21}$ cm$^{-2}$, then thin-target modeling is appropriate (Zirin 1988). Thus if the densities are $n_e \approx 3 \times 10^{10}$ cm$^{-3}$ and loop lengths are $L \approx 10^{10}$ cm, the thin-target analysis would be correct.

A downward streaming electron beam would result in forward peaked bremsstrahlung. Redirection by subsequent Compton scattering would tend to wash out this effect selectively at lower energies. One can measure this directional emission signature in three ways: (a) search for limb

clustering of $\gamma$-ray flares (Vestrand et al 1987); (*b*) look for trends in the spectral index of flares as a function of heliocentric angle (Vestrand et al 1987); and (*c*) measure the spectral index of the same flare simultaneously from two different viewing angles (Kane et al 1988). Simultaneous *PVO* and *ISEE* flare observations do not indicate any systematic anisotropy, whereas the other two methods support directionality (see Bai 1988).

HXR ($>10$ keV) bursts during the impulsive phase of flares have long been interpreted as evidence of 10–100 keV electron beams resulting in bremsstrahlung (Lin & Hudson 1971), following the thick-target model of Brown (1971). Two difficulties with this model [see also Alexander (1990)] are that: (*a*) very strong neutralizing reverse currents should occur, which could choke off the beam, and (*b*) the number of electrons required is uncomfortably close to the number available in the coronal region of acceleration. The measurement of $\gamma$ rays along with some HXR flares betrays the presence of energetic ions, and so the possibility arises that ion beams (in particular, proton beams) may carry the major fraction of the flare energy (Simnett 1986). If HXR bursts result from an electron beam, the mean particle energy required is $\sim 30$ keV; if it is a proton beam, the energy requirement rises to $\sim 200$ keV (Martens & Young 1990). [See Brown et al (1990) for a review of the electron vs proton beam models.]

Above 10 MeV, protons outnumber electrons by as much as a factor of 100. However, the production of X-ray bremsstrahlung results from 10–100 keV particle beams. At issue is whether protons are important at these lower energies (Martens 1988). Simnett (1986) makes several arguments for proton beams.

1. Nonthermal electron-ion bremsstrahlung has a very low efficiency, ($<10^{-4}$). Thus the energy in the electron beam giving rise to the HXR burst must be at least $10^4$ times that of the hard X rays. However, this estimate refers only to the energetic electrons above, say, 20 keV. If the power law distribution of electrons continues to rise steeply ($N(E) \propto E^{-4.5}$), even more flare energy is required for the more abundant lower energy electrons, so that the ratio of electron beam energy to HXR burst energy is too large.

2. Rapid, significant chromospheric evaporation requires deeper heating and hence more hard X rays than electron beams can provide.

3. The correlation of UV bursts with HXR bursts would also appear to require heating at densities of $\approx 10^{14}$ cm$^{-3}$, again beyond the reach of electron beams.

4. Hard X rays sometimes lead microwaves (by up to 5 s); delays should be the other way around. [However Lu & Petrosian (1990) propose some possibilities (see also Nitta & Kosugi 1986).]

On the stellar front, Grinin & Sobolev (1988, 1989) have presented a calculation of production of optical flares by proton beams. If protons and electrons have the same velocity, the protons will be 1800 times as energetic, hence penetrate much further into the chromosphere and photosphere, effectively producing optical radiation.

Proton beams resolve some problems but HXR bremsstrahlung could still be produced by thermal electrons. Simnett and Haines claim to have such a model in which "collective plasma effects may cause significant energy transfer from the ions to electrons, which in turn produce the X-rays via bremsstrahlung" (see Simnett & Haines 1990, Simnett et al 1989). Heristchi (1986), following up on Boldt & Serlemitsos (1969), has, however, developed a model in which protons directly produce HXR bremsstrahlung. The term bremsstrahlung (simply German for *brake radiation* and spelled in various remarkable ways by English language authors) usually refers to braking of fast electrons by slow ions, but other interactions are possible, specifically fast proton braking by ambient electrons; this type of proton-electron bremsstrahlung has also been called inverse bremsstrahlung. Such proton beams would give rise to certain specific $\gamma$-ray lines via nuclear capture of the protons and subsequent radiative deexcitation of excited states (MacKinnon 1989).

## 5.6 *Difference Between Solar and Stellar Radio Flare Mechanisms*

Although solar analogy can plausibly account for all the other radiations seen in stellar flares, it cannot do so for the highly polarized, high brightness-temperature radio flares that appear to require a coherent emission mechanism (such as plasma emission or cyclotron maser emission; Winglee & Dulk 1986) fundamentally different from that seen on the Sun (see Lang et al 1983, Dulk 1985, Jackson et al 1989). As summarized by Dulk (1987), the following properties separate the incoherent (probably gyro-synchrotron) from the coherent cm-wavelength dMe radio events: (a) time scales ~ seconds to minutes, polarization $\leq 30\%$, broad band $\Delta f/f \geq 0.1$, source size ~ $1R_*$, $T_B \leq 10^{10}$ K; (b) time scales ~ milliseconds to seconds, polarization $\geq 90\%$, narrow band, $\Delta f/f \leq 0.01$, source size unresolved, $T_B \geq 10^{12}$ K. The latter could be versions of the millisecond radio spikes seen on the Sun, which are restricted to time scales less than 100 ms in duration, but otherwise are similar in terms of being narrow band and having very high brightness temperatures [up to $10^{15}$ K (Benz 1986)]. On the other hand, highly polarized, narrow band stellar events can last for several hours, unlike anything observed on the Sun (Lang & Willson 1986, 1988).

In the solar case, bursts of hard X rays and microwaves are well correlated, and soft X rays are often (but not always) associated with gradual-riseand-fall microwaves. SXR-microwave correlations were not seen in several stellar flares observed simultaneously with the VLA and *Exosat* by Kundu et al (1988); nor were there correlations between the general radio and general X-ray variability. In fact, radio flares are not always associated with any other electromagnetic emission, again attesting to possible important differences between the solar and stellar situations. The study by Spangler & Moffett (1976) indicates only a moderate tendency for radio and optical flares to be associated within ± 10 minutes, suggesting highly beamed coherent synchrotron emissions, that may explain null radio detection, or inadequate detection limits. More recent observations show almost simultaneous enhancements of optical and microwave fluxes for the most intense flares (Rodonò et al 1984, Rodonò 1986a, Rodonò et al 1989).

Lastly, broad-band stellar quasi-periodic fluctuations (*pulsations*) have been reported (see for example, Bastian et al 1990). These may be MHD oscillations in a magnetic loop.

## 5.7    *The Two-Ribbon vs Compact Flare Categorization*

The concept has developed of a dichotomy between flares that are small in energy ($\sim 10^{30}$ ergs), short in duration ($\sim 10^3$ s), and confined to a single loop (compact flares); and events that are more energetic ($\sim 10^{32}$ ergs), of long duration ($\sim 10^4$ s), and involve the evolution and release of energy in an entire arcade of loops (two-ribbon flares) (Pallavicini et al 1977). Compact flares always occur along magnetic neutral lines and either peak in the optical in less than 30 s or continue to rise in brightness at a very rapid rate. Two-ribbon flares, on the other hand, are associated with filament eruptions and have multiple rises and dips in their light curves that may last for hours. Such a dichotomy is undoubtedly an oversimplification (Poletto 1989, Svestka 1989), and Pearce & Harrison (1988) argue that it is wrong altogether.

Although some argue that flare energy release cannot occur in a single loop (see Uralov 1990), it is useful to conceptualize the flare processes taking place in an energized single loop and to think of a two-ribbon flare as a sequence of reconnections and energy releases taking place in higher and higher magnetic loops in an arcade triggering a series of compact flares. (See Vrsnak et al 1987 and the evidence for multiple sequential excitations of Neupert 1989.) This picture for the two-ribbon flare interprets the spreading of Hα brightenings (ribbons) as heating at the footpoints of ever larger loops, loops which eventually appear as dark Hα structures out of which cooling material drains.

Kopp & Poletto (1984) have developed a simplified analytical model for the two-ribbon flare reconnection process. Interestingly Poletto et al (1988) have applied this model to the same 1980 Prox Cen flare that Reale et al (1988) successfully modeled in the compact flare paradigm. [This same event observed by Haisch et al (1983) was also recently reanalyzed by Byrne & McKay (1990); it appears that this *Einstein* X-ray light curve has the same *flair* for showing up in presentations as the ubiquitous *Skylab* false color "boot of Italy" coronal hole.]

# 6.   THE ANALYSIS OF FLARES

## 6.1   *Flare Energy Budget*

One would like to trace all the energetic processes in a flare to some common origin likely to be localized at some unresolvably fine scale in the magnetic field. However, we are not yet sure that all possible energy routes have been identified. Bornmann (1987), for example, argues that line profiles imply that a major fraction of the flare energy may temporarily reside in turbulent motions, as a sort of reservoir until the cascade from large- to small-scale eddies converts this into thermal energy.

Bruner & McWhirter (1988) have calculated that over the full range of solar conditions there is a simple relationship between total emitted power in the C IV doublet and the total radiative losses: $L_{tot} \approx 6 \times 10^3 L_{C IV}$. The ratio $L_{tot}/L_x$ (*Einstein* IPC, *Exosat* LE) is in the range $\approx 2$–10 for coronal plasmas (Doyle 1989, Haisch & Simon 1982). Taking $L_{tot}/L_x = 10$ for a very hot flare, the Bruner & McWhirter relation would predict $L_x/L_{C IV} \approx 600$. Checking this estimate against the 1980 Prox Cen flare (Haisch et al 1983), we find that the energy emitted in C IV was $E_{C IV} \approx 7 \times 10^{29}$ ergs, and the X-ray energy amounted to $E_x = 2.5 \times 10^{31}$ ergs, yielding $E_x/E_{C IV} \approx 35$, different from the prediction by a factor of 20.

Regarding the EUV continuum, Cheng & Kjeldseth Moe (1978) determined that $E_{EUV} \approx E_x$ in a solar flare. The dearth of EUV observations and the discrepancy between prediction and measurement in the Prox Cen flare point to the present difficulty of even achieving a proper energy budget for the radiation, much less other energy channels.

The largest solar flare ever studied involved $E \sim 2 \times 10^{32}$ ergs (Gershberg 1989). Several large flares on dMe stars involved $E \sim 10^{34}$ ergs (YY Gem, Doyle & Mathioudakis 1990; Gl 890, Byrne & McKay 1990; a 1969 observation of YZ CMi, Andrews 1990). The record event may be the enormous flare of more than 7 magnitudes (photographic, hence probably greater in the *U*-band) observed by Bond on the dM4e AF Psc, for which $E \sim 4 \times 10^{35}$ ergs was estimated (Greenstein 1977). Even more energetic flares occur on the RS CVn stars. On II Peg, total radiative losses in one

flare were estimated [from the C IV Bruner & McWhirter (1988) relation] to be $E \sim 2.4 \times 10^{36}$ ergs (Doyle et al 1989). In the HR 1099 flare reported by Linsky et al (1989), the ultraviolet losses alone amounted to $2.4 \times 10^{36}$– $3.6 \times 10^{36}$ ergs. Pye & McHardy (1983) identified six *Ariel V* fast transient (several hours in this context) X-ray events with RS CVn flares, and derived energies up to $3 \times 10^{37}$ ergs in the 2–18 keV band. Allowing for unobservable nonradiative processes, we estimate that the total flare energy may exceed $10^{38}$ ergs in the largest RS CVn flares.

## 6.2   *Magnetic Field Measurements*

The MSFC vector magnetograph (Hagyard 1990) measured approximately $10^{32}$ ergs of total stored nonpotential energy above an active region (Gary et al 1987). This is only a $3\sigma$ measurement, so improvements are necessary before we can measure the change in field and equate that to the total energy involved in the flare. Another use of vector magnetograms consists of identifying regions of vertical current flow, $J_z$, through the photosphere and correlating these sites with flare footpoints. Hagyard (1988) did find such $J_z$ concentrations precisely at regions of repeated flaring. Such observations demonstrate that the presence of sheared photospheric magnetic fields, rather than just concentration of vertical (line-of-sight) field, results in flares (Hagyard 1990).

Concerning stellar magnetic field measurements, Hartmann (1987) states: "Although hundreds of papers have been written on stellar magnetic activity, only a few have actually been devoted to measuring stellar magnetic fields." All stellar measurements involve excess broadening of line profiles as a result of the Zeeman effect because other techniques used on the spatially resolved Sun cannot work on point-source stars where signatures of opposite polarity cancel. Therefore, one must be confident (or naive) in one's belief that all parameters determining the line profile are known and can be modeled to extract the Zeeman contribution. In principle, one can derive both the mean field strength and the mean surface coverage by using a technique such as that of Robinson et al (1980). As to the very existence of flare-producing magnetic fields on stars, we take heart in the conclusion of the Basri & Marcy (1988) study that: ". . . magnetic fields are really being detected." For example, evidence is good for a 1000 G field covering 35% of the surface of $\varepsilon$ Eri, a 1200 G field covering 40% of $\xi$ Boo A, and a 3800 G field covering 70% of AD Leo (Saar & Linsky 1985; see Linsky 1989 for a review). Also, indirect evidence suggests saturated levels of magnetic activity in some stars (Vilhu et al 1989).

Saar & Linsky (1985) and Saar et al (1986) have improved the Robinson technique by avoiding systematic errors deriving mainly from the presence

of weak blends in late-type star spectra and the lack of radiative transfer treatment [cf Hartmann 1987, Saar 1987; see also Linsky (1989) for a summary of some of the critical issues involving use of the Robinson (1980) technique]. A large body of data on the magnetic field strengths and filling factors for late dwarfs is now available (Saar 1988); reasonably credible magnetic mapping has even been done for $\xi$ Boo A (Saar et al 1988).

## 6.3  *Multispectral Stellar Observations*

*Exosat* observations of flare stars involved 300 hours of monitoring 22 stars resulting in 32 flares. Examination of this data base (Pallavicini et al 1990b) revealed examples of stellar analogs for the two different types of flares—compact and two-ribbon—seen on the Sun (Pallavicini et al 1977): *impulsive flares*, which are like solar compact flares, and *long-decay flares*, which are like solar two-ribbon flares (see the discussion in Section 5.7). They also found both types occurring on the same star.

Time resolution ($\approx 1$ m) is now possible at a spectral resolution of approximately 2000. The following features generally characterize the emission line flare behavior (Houdebine et al 1991, Zirin & Tang 1990, Rodonò et al 1989): 1. He I lines rise rapidly and follow the *U*-band light curve. 2. The H Balmer lines tend to lag behind; H$\gamma$ is inevitably the strongest line of the series. 3. The Ca II H and K lines lag still farther, typically peaking 5–15 minutes after the flare onset. 4. The Mg II lines have the slowest response, but enhancements may persist for several hours following the optical continuum flare. Time-resolved lines have been used to determine cooling curves for the $10^4$–$10^5$ K plasma (Houdebine et al 1991), yielding $n_e \sim 10^{12} \, \mathrm{cm}^{-3}$.

A 2-mag flare in the *U*-band observed on AD Leo was observed simultaneously with *IUE*, the VLA, and several optical telescopes (Rodonò et al 1989) as shown in Figure 5. Note the following. 1. Simultaneous IR *K*-band photometry (2.2 $\mu$) showed dips during this flare, the missing energy amounting to about 7 times the excess *U*-band flux. This would imply approximate equality between the missing IR flux and the total excess emission in all bands. 2. The H$\gamma$ line showed a blueshifted component implying velocities of 6000 km s$^{-1}$ near flare maximum and a total kinetic energy of $5 \times 10^{34}$ ergs. This mass loss episode resembles solar CME events, but is a factor of 500, 40, and 4 times more intense as far as the total energy involved, the amount of mass loss, and the mass ejection velocity, respectively, are concerned. Houdebine et al (1990) estimated a total mass loss that could affect the normal evolution of such flare stars.

Using time-resolved, multicolor photometry, deJager et al (1989) derived a color temperature ($T \approx 16,000$ K) for an optical flare on UV Ceti, and,
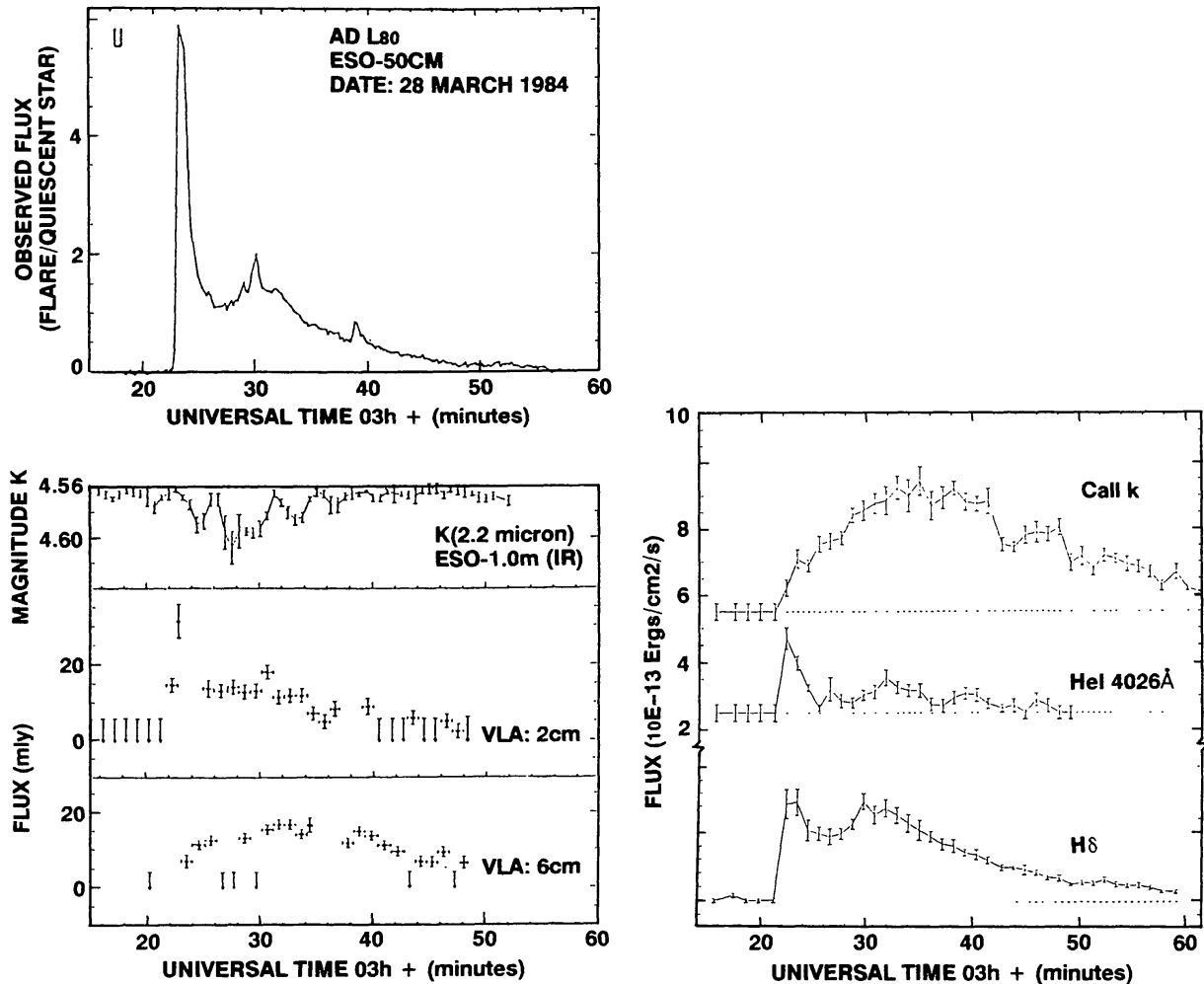
*Figure 5*   Multispectral observations of a flare on AD Leo showing the time history of the U-band, lines, IR, and radio measurements. Note the K-band dip (from Rodonò et al 1989).

with absolute photometry, an area. This event peaked at $L \sim 1.8 \times 10^{30}$ ergs s$^{-1}$ between 3200–5000 Å. The optical flare footpoint(s) comprise an area of 9000 km effective diameter at the outset, decreasing to 3000 km after 5 min. On the Sun, this would be $\approx$ 5–15 arcsec, hence very analogous. However, a big difference is the vertical extent of the flare transition zone, which analysis suggests is 50 times that of the solar case, with a plasma density 100 times solar. The X-ray observations show a multithermal hot plasma ($T \sim$ 10–40 MK) whose total mass could have explosively evaporated into the corona in the first 30 s or so of this event.

## 6.4  *Plasma Emissivity*

Knowledge of the plasma radiative properties is important. Determining the flare energetics requires a radiative loss function, $\Lambda(T)$, which specifies

the cooling as a function of temperature for optically thin emission. Observations always cover a limited spectral range, and so the overall energy budget requires corrections for the radiation out of the passband. In addition, the presence, strengths, and ratios of lines may be used to determine the temperature and emission measure provided individual line emissivities are known.

Several dozen major computational models have been published starting with the solar-oriented work of Elwart (1961). These now have much wider application ranging from stellar coronae and flares to galactic halos. Two large modern compendia are the programs of Mewe et al (1985) and Landini & Monsignori Fossi (1990); extensive bibliographies of prior efforts may be found therein. These codes are applicable to hot plasmas of $10^4$–$10^8$ K and optically thin lines and continua in the 1–2000 Å (Landini & Monsignori-Fossi) range (see Figure 6). A cosmic abundance is assumed. Continuum processes include free-free (electron-ion bremsstrahlung), free-bound, and two-photon from H-like ions.
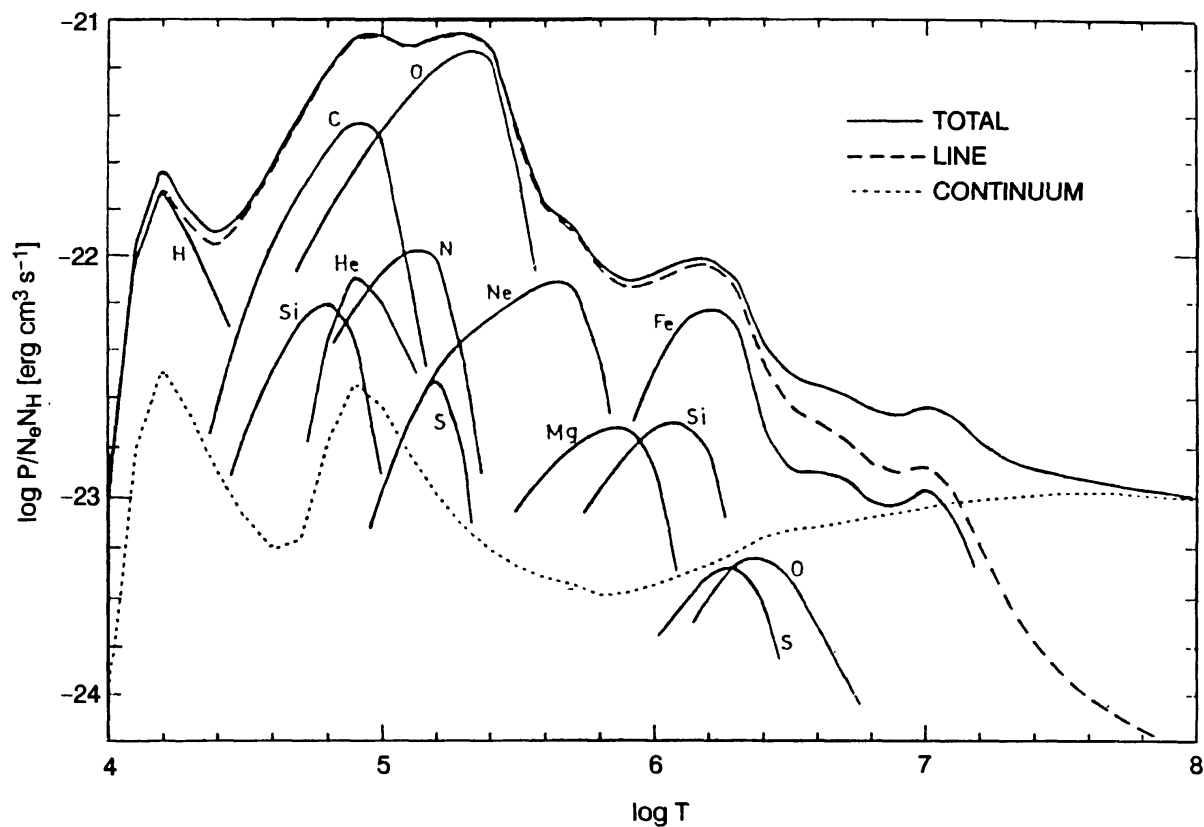


*Figure 6* The total emissivity and contributions from individual elements in the 1–2000-Å spectral region (from Landini & Monsignori-Fossi 1990).

## 6.5   Conditions in the Flare Loops

Solar flare temperatures were originally derived from proportional counter pulse height spectra by *OSO-7* in 1971–72 (Datlowe et al 1974). More recently, flare temperatures have been derived from X-ray Bragg crystal spectrometer line measurements on *P78-1*, *SMM*, and *Hinotori*. This line method is based on determination of the ratio of a dielectronic satellite line to a resonance line from the same ionization stage, and so is not restricted by ionization equilibrium assumptions (Gabriel 1972). During flares, H-like (e.g. Mg XII, Ca XX, Fe XXVI) and He-like (e.g. Fe XXV, Ca XIX) ions dominate the spectrum, and unfortunately these lines have a very broad temperature of formation. Doschek & Feldman (1987) analyzed in detail the sensitivity of these types of temperature determinations to the presence of multitemperature plasmas.

Flare temperatures are derived from the ratios of dielectric recombination to electron impact excitation lines. Detailed considerations of the emission measure and contribution function of various ions (Doschek 1990) indicate that the peak temperatures for flares greater than about M5 lie in the range 20–30 MK. Such a narrow range of maximum temperature is a surprising and significant finding given the tremendous differences in time and length scales involved. However, a superhot component does manifest itself both in Fe XXVI emission and in small HXR bursts, with $T > 35$ MK.

A flare apparently has two distinct thermal components (Lin et al 1981, Tanaka 1986): a long-lived, gradually rising and falling component that is predominant in the emission measure and lies in the range $T \approx 13$–25 MK; and a superhot component arising near the peak of the HXR burst that appears to be located at the tops of the coronal loops, and has a temperature $T \approx 30$–40 MK. The analysis of Doschek & Feldman (1987) indicated that, if only H-like and He-like lines are used, plasmas as hot as several hundred million degrees would escape detection—even with emission measures on the order of 10% of the main thermal component. Direct observation of the spectral energy distribution, as done in the Lin et al experiment, requires considerable energy resolution.

The differential emission measure, $DEM(T) = n_e^2(T) \, dV/dT$, is an important parameter characterizing the optically thin emitting plasma above $10^4$ K. If $T(z)$ is assumed to be a monotonically increasing function, then it is convenient to consider the *DEM* of a vertical cylinder of unit area, $DEM = n_e^2(T) \, (dT/dz)^{-1}$. It is a curious fact that although this *DEM* (per unit area) may vary in absolute value by a factor of 1000 from quiet Sun to flare, the general shape is approximately the same everywhere (see Bruner & McWhirter 1988—note that they show Emission Measure, which scales as $EM \propto DEM \cdot T$). For $T < 10^5$ K, $DEM \propto T^{-3.5}$; above that

temperature $DEM \approx$ constant. Moreover, the stellar $DEM$ appears to have the same universal shape.

Typical flare densities in the corona lie in the range of a few times $10^{10}$ to a few times $10^{12}$ cm$^{-3}$ (Doschek 1990, Brown et al 1985). The most extreme measurements of coronal densities (about $4 \times 10^{12}$ cm$^{-3}$) have come from the use of the ratio of the forbidden and intersystem lines of He-like Ne IX and Mg XI (Wolfson et al 1984, Linford & Wolfson 1989). The combination of the density and emission measure determination during such flares makes possible the determination of the volume of the emitting plasma; comparing this to the size of the field of view gives a filling factor for the coronal plasma. The filling factors of the high temperature flare component appear to be very small ($\leq 0.01$), implying that the structure of the flare is highly filamentary. Linford et al (1988) derived an upper limit of less than 0.5 arcsec (about 350 km) for the diameter of a loop in a short-lived compact flare. (This study was done with a relatively low resolution spectrometer, which is encouraging with regard to stellar possibilities using proper diagnostics.) The transition region flare plasma appears to have a very small filling factor, as expected in the context of flaring loop models with (vertically) expanding geometries (Doschek 1990).

The first spectroscopic evidence for abundance variations during flares was reported by Sylwester et al (1984) based on BCS observations of Ca XIX by *SMM*. Further evidence for this phenomenon has been found even in quiescent active regions (Strong et al 1990). Variations of about a factor of four have been observed in some elemental abundances in the corona. Further confirmation of this variation came from the analysis of *Skylab* data (Widing & Feldman 1989), in which even higher variability was found. Meyer (1985a,b) has pointed out the observational diversity of abundance measurements in the corona and cosmic rays. He associates this with the first ionization potential (FIP) of the element. The higher the FIP of a given element, the larger is the range of temperature over which it is neutral and thereby able to diffuse easily across the magnetic field. Hence, elements with high FIPs, such as helium and neon, can build up a different abundance distribution from elements that are less mobile (i.e. have a lower FIP). This has important implications for the analysis of line spectra from a plasma: If the elemental abundance changes by these large factors, then estimates of temperatures (from line ratios), emission measures, and energetics will be unreliable. Hence, one must determine the local abundance of the plasma before making such measurements.

## 6.6 *Cooling Curve Analysis*

The decay time of a flare has been used to describe many different things. Usually it refers to the equivalent initial exponential decline of a light

curve. This interpretation clearly poses a problem in the case of a spectral line or a spectral band in which the emissivity $[\Lambda(T)]$ may rise, or rise and then fall, as the temperature drops [e.g. Figure 14 of Haisch et al (1988) in which Mg XI would decrease in strength as $T$ drops below $10^7$, but Ne IX and O VIII would continue to rise until $T \approx 10^{6.5}$]. The important physical measurement concerns the energetics, and hence the time scale of the cooling rate, $d(3n_e kT)/dt$, matters most. In the derivation below, we follow the analysis of van den Oord et al (1988). (See also the technique of Svestka 1987.)

The conductive flux lost through the two bases (footpoints) of a loop of length $L$ is approximately $F_{c,b} = 2\kappa_0 T^{7/2}/L$; all the energy lost by conduction is therefore lost at the footpoints, $E_{c,b} = 2A_b F_{c,b}$, since internal redistribution of energy is not a loss. The average conductive loss per unit volume is thus $\langle E_c \rangle = E_{c,b}/V$. Assuming a linear increase in cross section, $\Gamma = A_{cor}/A_b$, one arrives at the expression for the mean conductive loss for a uniformly expanding loop, $\langle E_c \rangle = 8\kappa_0 T^{7/2}/(\Gamma+1)L^2$. The optically thin radiative loss is expressed by $n_e^2 \chi T^\alpha$ (e.g. Priest 1982), and the energy equation is then,

$$\frac{d}{dt}(3n_e kT) = -n_e^2 \chi T^\alpha - \frac{8\kappa_0 T^{7/2}}{(\Gamma+1)L^2}. \qquad 1.$$

We assume the following three initial exponential decays:

$$n^2 T^\alpha = n_0^2 T_0^\alpha \exp(-t/\tau_d), \qquad 2a.$$

$$T = T_0 \exp(-t/\tau_T), \qquad 2b.$$

and

$$nT = n_0 T_0 \exp(-t/\tau_{cool}). \qquad 2c.$$

The last of these may be rewritten in terms of the other two as,

$$(n^2 T^\alpha)^{1/2} T^{(1-\alpha/2)} = n_0 T_0 \exp\left[-\frac{t}{2\tau_d} - \frac{t}{\tau_T}\left(1 - \frac{1}{2}\alpha\right)\right]. \qquad 3.$$

Substituting these expressions into the differential equation for energy, and defining conductive and radiative cooling times as $\tau_{cond} = 3n_e kT/\langle E_c \rangle$ and $\tau_{rad} = 3n_e kT/n_e^2 \chi T^\alpha$, one can show that initially (at $t = 0$),

$$\frac{1}{\tau_{cool}} = \frac{1}{\tau_{rad}} + \frac{1}{\tau_{cond}} = \frac{1}{2\tau_d} + \frac{\left(1 - \frac{1}{2}\alpha\right)}{\tau_T}. \qquad 4.$$

## 6.7  Proton Beam Signatures

A signature of medium-energy ion beams was proposed by Orrall & Zirker (1976)—that is, Doppler-shifted Lα emission from protons picking up electrons on the way down; this effect was not seen in *Skylab* ATM data. A similar effect is expected in the He II Lα line at 304 Å, in which a redshifted component is predicted at 308–312 Å (Peter et al 1990). Impact linear polarization of chromospheric lines is another possible diagnostic of proton beams, in particular in Hα (Henoux et al 1990b). In fact, polarization as high as 2.5% in Hα has been observed in bright patches on the Sun. Abnormally low drifts in radio frequency with time during Type III bursts could also be indicative of proton beams (Benz & Simnett 1986).

Martens & Young (1990) summarized arguments for proton beams. They concluded that: 1. Significant energy deposition in the chromosphere is required prior to the onset of HXR impulsive emission to explain *SMM* Ca XIX turbulent line broadenings and high upflows; proton beams can generate such heating without producing X rays, whereas electron beams cannot. 2. Thick-target electron beams should result in anisotropic, polarized hard X rays, whereas stereoscopic observations indicate isotropy and low upper limits on polarization. 3. The simultaneity of impulsive hard X rays and $\gamma$ rays demonstrates the presence of high-energy protons ($> 30$ MeV).

# 7.  MICROFLARING AND CORONAL HEATING

## 7.1  Low Level Solar Flaring

The most rapid fluctuation observed in flares occurs in decimetric radio waves, in which spikes on time scales of a few milliseconds have been measured.

In hard X rays ($E > 20$ keV), the time profile of an individual flare event is dominated by rapid bursts during the onset phase. Often a plot of the integrated energy under the spiky HXR light curve as a function of time matches the shape of the SXR light curve. This result implies that the energy of the plasma radiating soft X rays is supplied by the same mechanism giving rise to the hard X rays, provided that the $\tau_{cool} \gg \tau_{heat}$.

The X-ray flares detected by *OSO-7* in 1971–1972 already demonstrated how the cumulative number of events increased as the flux level of the events decreased; Datlowe et al (1974) derived this result from an analysis of 123 HXR bursts. A balloon flight in 1980 significantly lowered the flux detection threshold (Lin et al 1984), and 25 HXR bursts were observed in

141 min. These new lower level flares confirmed the earlier conclusion that the number of events steadily increases as one includes smaller events, with $N(E > E_0) \sim E^{-1}$. The spectrum of HXR bursts also follows a fairly steep power law down to some cutoff. Therefore, depending on the power law index and the cutoff, the actual energy of a burst in the wavelength region $E > 10$ keV might be 10 times that measured above 20 keV. Thus, a reasonable estimate of the energy released in HXR bursts and microbursts (extrapolated below the Lin et al threshold and extrapolated to SXR energies) could conceivably approach the $L_x = 10^{27}–10^{28}$ ergs s$^{-1}$ of the entire solar corona.

Six of the 25 microflares observed by Lin et al (1984) were simultaneously detected in Hα by Canfield & Metcalf (1987). The Hα line profiles are consistent with chromospheric evaporation resulting from nonthermal electron beam heating. Athay (1984) and Porter et al (1984) found that frequent brightenings in transition region lines such as C IV, Si IV, and O IV occur in active regions, typically lasting 20–60 s with intensity increases of 20–100%, although much larger events are seen. The same behavior is found in the solar network (Porter et al 1987), where simultaneous magnetograms point to the brightenings taking place in small bipoles. A further link is made with the explosive events seen by HRTS spectrograms in C IV (Brueckner & Bartoe 1983). Parker (1988) uses these fluctuations to arrive at an estimate of $\approx 8 \times 10^{22}$ ergs s$^{-1}$ or $1.6 \times 10^{24}$ ergs (in a typical event) for each event, which he dubs a *nanoflare*. As in large-scale occurrences, turbulence and rapid flows are associated with these events, implicating the HRTS C IV events with nanoflaring. Porter et al (1987) argue that Hα spicules originate in such microflares. Perhaps most importantly, the occurrence rate (extrapolated from small areas) coupled with the energy per event, the location of events both in active regions and in the network, and the evidence for a continuous spectrum of events from flare to nanoflare (Athay 1984, Lin et al 1984, Parker 1988) have led to the proposition that the corona is heated by flares, microflares, and nanoflares.

Magnetic flux tubes are swept around by photospheric convective motions (shown in Figure 7) which should lead to spontaneous tangential discontinuities in the magnetic field (see Parker 1987 and his references pointing back to this concept in the early 1970s). This idea led Sturrock & Uchida (1981) to model the increase of magnetic free energy in the corona resulting from these stochastic motions and to compare this energy with coronal heating requirements; recent work by Zappalà & Zuccarello (1989) indicates that up to $10^{33}$ ergs of magnetic energy can be stored. Although it is not clear whether rotation of flux tubes results from this jostling of footpoints, translational motions of the flux tubes must wind
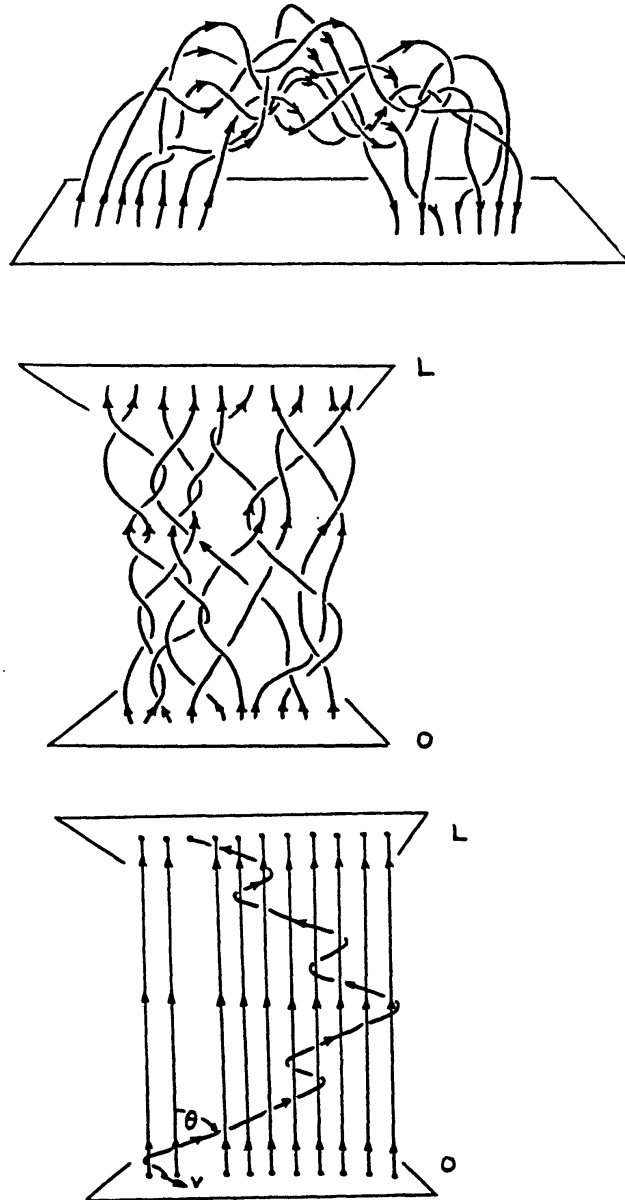
*Figure 7*  The "Parker Spaghetti" model of the motions of coronal field lines. (*Top*) The lines of force of a bipolar magnetic region; (*middle*) schematic of the version used for analysis; (*bottom*) the wandering of a single line of force driven by photospheric motions (from Parker 1988).

the coronal extensions of the magnetic field around each other. This winding does not necessarily result in energy release; however, as Antiochos (1987) has shown, current sheets will form either because the finite resistivity or the intrusion of new magnetic flux from below leads to local reconnections, which then result in flarelike coronal heating. In fact, flux cancellation appears to be a necessary condition for flare occurrence (Livi et al 1989).

Sturrock et al (1990) calculated the *DEM* averaged over space and time resulting from episodic heating and cooling of many loops; i.e. they examined whether the steady-state *DEM* function could be reproduced by an ensemble of time-varying (randomly heated) mini-flare loops (see also Raymond 1990); apparently it can. The steeply dropping portion between $10^4$–$10^5$ K is a direct result of the steeply rising emissivity, $\Lambda(T)$. However since $\Lambda(T)$ decreases with temperature above $10^5$ K, heating beyond this critical temperature would lead to a thermal runaway, were it not for conduction, which increases in efficiency as $T^{5/2}$. Conduction thus determines the shape of the *DEM* in the high temperature regime, and time- and space-averaged microflaring *DEM*s appear to reproduce the observed function.

The random walk of loop footpoints around each other induced by photospheric convective motions results in a steadily increasing horizontal (transverse) component of magnetic field. This action builds up stored magnetic energy as work is done against the stressed field: $W \approx B^2 v^2 t / 4\pi L$ (Parker 1988). Because the braiding of flux bundles is random, the helicity, $\alpha$, varies discontinuously along the loop giving rise to numerous current sheets. Parker argues that beyond a certain stress, rapid reconnection occurs with each reconnection event at each current sheet resulting in a nanoflare. Equating the coronal heating rate ($W \approx 10^7 \, \mathrm{ergs\,cm^{-2}\,s^{-1}}$) with work done by the footpoint motions, and making assumptions about the random walk characteristics, Parker estimates that typically 100 random steps characterize the buildup and that the region involved is the non-potential magnetic field within $V \approx 6 \times 10^{23} \, \mathrm{cm^3}$. On the assumption that the UV fluctuations of Porter et al (1984) correspond to clusters of nanoflares ($\sim 5$ assumed), Parker (1988) argues for an energy per nanoflare of about $1.6 \times 10^{24}$ ergs, with the event lasting about 20 s. This estimate is based on the assumption that 20% C IV fluctuations correspond to 20% fluctuations in the total power, i.e. $E_{\mathrm{nf}} = 0.2 \times 10^7 \times 4 \times 10^{16} \times 20$. If such an event has the differential emission measure typical of hot solar loops, then C IV and total power have a constant relation: $E_{\mathrm{tot}} \approx 6 \times 10^3 \times E_{\mathrm{C\,IV}}$ (Bruner & McWhirter 1988). On the other hand, if nanoflares are not simply scaled-down flares, the energy estimate may be very far off.

The number of flares versus power (or energy flux) per event appears to follow a power-law distribution, $dN/dP = kP^{-\alpha}$. Integrating the expression, we arrive at the equivalent cumulative distribution, $N(>P) = kP^{1-\alpha}$. Often a similar expression is cited in terms of energy rather than energy flux, but usually the energy flux is implied even though it is stated as energy; the power law in terms of energy and energy flux could only be the same if the duration of a flare were energy independent,

which is not the case. Hudson (1991) argues that $\alpha \approx 1.8$ for the total power in both the solar and stellar case for flares above some threshold: Important derivations of this power law for the Sun include the early work of Drake (1971) and Datlowe et al (1972) and the recent measurements of Lin et al (1984) and Dennis (1985); stellar data are numerous and have been summarized by Shakhovskaya (1989) in her Figure 2. Note that $k$ varies enormously from star to star and over the solar cycle, but the occurrence distribution, $\alpha$, is the important constant factor.

A simple conclusion can be drawn concerning the flare-driven luminosity:

$$L_{\mathrm{f}} = \int_{P_{\min}}^{P_{\max}} \frac{dN}{dP} P \, dP, \qquad\qquad \text{5a.}$$

which after integrating yields

$$L_{\mathrm{f}} = \frac{k}{2-\alpha}[P_{\max}^{2-\alpha} - P_{\min}^{2-\alpha}], \quad \text{for } \alpha < 2 \qquad \text{5b.}$$

and

$$L_{\mathrm{f}} = \frac{k}{\alpha-2}\left[\left(\frac{1}{P_{\min}}\right)^{\alpha-2} - \left(\frac{1}{P_{\max}}\right)^{\alpha-2}\right], \quad \text{for } \alpha > 2. \qquad \text{5c.}$$

The last two expressions are the same algebraically, but are written to make clear that in the first case ($\alpha < 2$) $L_{\mathrm{f}}$ is determined by the most powerful flares less the microflares. The lower the level of microflaring, the more this subtractive term goes to zero, increasing $L_{\mathrm{f}}$, but the maximum of $L_{\mathrm{f}}$ is determined by $P_{\max}$. Only if $\alpha > 2$ is $L_{\mathrm{f}}$ determined by the inverse term of the least energetic microflares, i.e. the increasing number of smaller flares outweighs their decreasing power in contributing to integrated power. After calibrating the total power from single-band distributions, Hudson (1991) demonstrates that microflares following an $\alpha \approx 1.8$ power law cannot contribute significantly to coronal heating.

## 7.2 Low Level Stellar Flaring and Coronal Luminosity Relations

Using *Exosat*, Butler et al (1986) reported on observations of short-time-scale variability in the 0.1–2 keV band light curves of two flare stars: UV Ceti and EQ Peg. In the case of UV Ceti, correlations were found between the X-ray and H$\gamma$ fluctuations as shown in Figure 8. These microflares are actually fairly large by solar standards, involving energies $E \sim 2 \times 10^{30}$ ergs and lasting from several tens of seconds to several minutes. They therefore resemble solar compact flares much more than the solar micro-
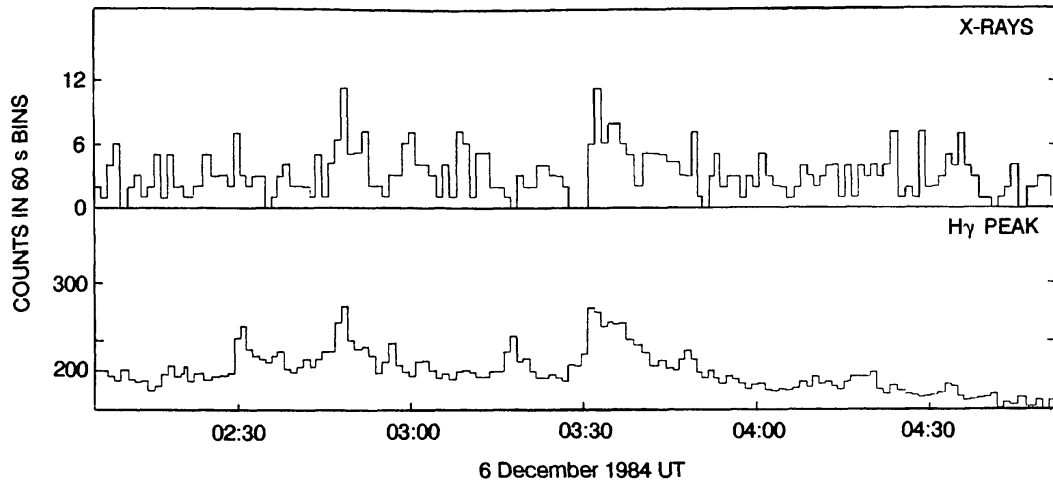
*Figure 8*   The SXR flux of UV Ceti as measured by *Exosat* versus $H_\gamma$ peak as seen by the ESO 3.6-m telescope (from Butler et al 1986).

flares ($E \sim 10^{27}$ ergs) or nanoflares ($E \sim 10^{24}$ ergs) of Parker (1988). They are also similar in energy to the solar active-region loop brightenings—which neither reached flare temperatures nor manifest $H\alpha$ emission—studied by Haisch et al (1988).

The statistical analyses of *Einstein* data on 19 stars by Ambruster et al (1987), and the similar study of 12 stars observed by *Exosat* (Collura et al 1988, Pallavicini et al 1990b), appear to support the occurrence of only moderate-level flaring on time scales of over 500 s, i.e. events that are more like subflares or moderate flares than microflares. A comprehensive survey of X-ray emission from neighborhood flare stars observed with *Exosat* has been carried out (Pallavicini et al 1990b). They confirm the known result that the X-ray luminosity of flare stars span over a wide range ($L_x = 10^{27}$–$10^{30}$ ergs s$^{-1}$) with no obvious dependence on the stellar rotation rate, but strong dependence on the star dimension. These results may indicate a saturation effect on the activity level. Substantial variability in X rays is also confirmed in the form of flares on time scales of tens of minutes or hours, but no evidence of microflaring is suggested (Butler et al 1986, Holman 1987, Butler et al 1988, and Mathioudakis & Doyle 1990).

Moffett (1972) was the first to detect rapid (0.3 mag s$^{-1}$) short-lived events (2 to 3 s) superimposed on stellar flare light curves. A system capable of $3 \times 10^{-7}$ s time resolution has been used at the Soviet 6-m telescope to monitor several flare stars (Beskin et al 1989a,b). The shortest flare observed had a rise time of 0.3 s and a duration of 1.7 s. The energy of such flares is in the range of solar subflares. The total energy of optical fluctuations does not exceed that of individually detected flares.

Two temperature fits to stellar coronal X-ray emission have consistently resulted in a flarelike component even at apparently quiescent times—pointing to ongoing microflaring—in some RS CVn and dMe stars. Swank et al (1981) first found this component in *Einstein* SSS spectra of eight RS CVns, indicating a $T \approx 20$–$100$ MK component. Agrawal et al (1981) later found a $T > 35$ MK component in an *Einstein* SSS spectrum of the RS CVn binary $\sigma$ Cor B. Swank & Johnson (1982) found similar evidence ($T > 10$ MK) in the SSS spectrum of the dM3.5e star Wolf 630 AB. A $T \approx 12$–$15$ MK component was found in IPC spectra of the dM2e star Gl 867A (Agrawal 1988). The detection of quiescent *Exosat* ME band emission in some flare stars points to a $T > 10$ MK component (Pallavicini et al 1990b). The *Exosat* filter ratio data on M dwarf stars also indicates the presence of $T > 10$ MK gas (Schmitt & Rosso 1988, Pallavicini et al 1988).

The quiescent $L_x$ of dMe flare stars range from $4 \times 10^{26}$ ergs s$^{-1}$ (Prox Cen; Haisch et al 1983) to $4 \times 10^{29}$ ergs s$^{-1}$ (YY Gem; Haisch et al 1990a). The X-ray variability for individual stars is not known; whereas Prox Cen appears to vary by as much as a factor of four (Haisch et al 1990b), multi-epoch observations indicate a more typical factor-of-two variability in the quiescent level (Pallavicini et al 1990b).

The M dwarfs deviate from the UV line vs SXR flux-flux relationships of F-, G-, and K-stars (Rutten et al 1989). They also do not appear to follow the Pallavicini et al (1982) rotation-activity relation; instead they show an $L_x \propto L_{\text{bol}}^{1.2}$ relationship (Pallavicini et al 1990b, Agrawal et al 1986). A correlation also appears between peak flare luminosity and quiescent stellar X-ray luminosity (Pallavicini et al 1990b). This is partially a selection effect, because only bright flares can be detected above a high background, but the existence of an upper envelope in the relationship does indicate that stars of low $L_x$ have relatively weak X-ray flares; in the case of Prox Cen (one of the stars with the lowest quiescent $L_x$), the observed X-ray flares are in the range of the very brightest solar flares.

Three independent studies (Whitehouse 1985, Doyle & Butler 1985, Skumanich 1985) arrived at the conclusion that $L_x \propto \langle L_{\text{U,f}} \rangle$, where $\langle L_{\text{U,f}} \rangle$ refers to a time-averaged, equivalent *U*-band flare luminosity (Haisch 1986). Skumanich (1986) claims that the time-averaged solar WLF power and quiescent coronal $L_x$ (at solar maximum) both satisfy this same relation. (Of course, the solar $L_x$ varies by about an order of magnitude over the 11-year cycle.) Two other correlations have been claimed: an inverse correlation between a star's flaring rate and $L_x$, and an inverse correlation between the flaring rate and the mean flare power. Harrison et al (1988) have tested these proposed stellar relations against solar active regions, with mixed results.

# 8.  MISCELLANEOUS TOPICS

## 8.1   *Solar Flare Periodicity*

The Sun exhibits quasi-periodic activity cycles affecting flare occurrence. The most obvious example of this is the 11-year solar cycle. Similar long-term cycles have been found on other stars (Baliunas & Vaughan 1985), but no relation to stellar flare cycles is yet possible.

The initial suggestion that the Sun exhibited "intermediate term epochs" of activity was made by Bouwer (1983) who found a variety of periodicities ranging from 80–160 days in *GOES* data for 1977–1981. A 154-day periodicity was discovered in the occurrence of 139 HXR/$\gamma$-ray flares observed by *SMM* and 532 SXR flares greater than M2.5 observed by *GOES* from 1980–1983 (Rieger et al 1984). Following this discovery, Bogart & Bai (1985) analyzed microwave flares from 1966 to 1983 (cycles 20 and 21) and found a 152-day periodicity that appeared to be phase coherent between the two cycles. Ichimoto et al (1985) also found this periodicity in H$\alpha$ flares from 1964 to 1983. Next, Bai (1987) investigated the occurrence of 443 major flares based on a comprehensive flare index (CFI) during cycle 19 for the years 1955 to 1969, and found a periodicity of 51 days, i.e. one third of a 153-day periodicity. Since then, the sunspot blocking function, the sunspot number, sunspot area, and the 10.7-cm radio flux were found to have a 155-day periodicity (Lean & Brueckner 1989, Carbonell & Ballester 1990). Dröge et al (1990) have found strong evidence for a 153-day periodicity in the occurrence of energetic solar electron events—measured in situ by the *ISEE 3* spacecraft—during 1978 to 1982; Gabriel et al (1990) found a 154-day periodicity in solar proton events during the past three solar cycles. However, none of the major periods of flaring during 1983–1988 seemed to be related to the 155-day periodicity. Attempts to use it as a predictive tool to organize *SMM* observing campaigns were fruitless. A much lower level and shorter periodicity (about 90 days) seemed to be established during this solar minimum period (K. T. Strong, unpublished data). Preliminary analysis of X flares during cycle 22 suggests a return of a 154-day periodicity phase-linked to cycle 21 (Brueckner & Cook 1990).

## 8.2   *Stellar Postflare Quasi-Periodic Oscillations*

Short-duration quasi-periodic ($\approx 10$–$20$ s) light oscillations beginning after the onset of an intense flare on the Hyades star II Tau ($=$ H II 2411) were reported by Rodonò (1974). Mullan (1976) suggested electron cyclotron waves (whistlers) traveling from one magnetic footpoint to the other as the cause of the observed oscillations. Rapid oscillations at radio wavelengths were reported by Gary et al (1982), who proposed a cyclotron

maser mechanism acting on an excited region at $T_b \gg 10^{12}$ K. Additional discussion may be found in Gibson (1983) and Lang (1990).

Houdebine & Foing (1991) studied the oscillatory behavior of Balmer line shifts during the late decay phase of a flare on AD Leo—observed with high time and spectral resolution by Rodonò et al (1989)—and suggested that the oscillations might result from periodic motions of a prominence with minimum radius and magnetic field strength of $2 \times 10^9$ cm and 20 G, respectively. Andrews (1989a,b, 1990a,b) and Andrews et al (1990) have found quasi-periodic fluctuations in the $U$-band with periods on the order of 10–40 s following optical flares for up to 15 min.

Although we cannot yet determine whether or not the effect is real, the possibility of having seen quasi-periodic variations in $U$-band photometric data is exciting because it could either be evidence for resonant heating oscillations in coronal loops in the context of the electrodynamic coupling theory (Ionson 1982, Mullan 1984) or indicate reprocessing of radiation in circumstellar disks or shells.

## 8.3  Sympathetic Flaring

The observation that flaring at one site leads to flaring at distant locations (perhaps as much as 90 degrees away) has given rise to the concept of sympathetic flaring. The phenomenon is not universally recognized. Pearce & Harrison (1990) studied activity in various pairs of active regions and found correlations for active regions that are relatively close (30 degrees or less), but their statistics indicate less correlation than expected on the basis of random occurrence for more widely separated pairs, which casts some doubt on the methods. Large-scale interconnecting loops have been known since *Skylab*, and filaments can span half the solar diameter; so means for triggering are present, but how much this actually happens remains an open issue.

Stellar flare statistics indicate that the flare occurrence distributions are not compatible with Poisson statistics for intervals below about 10 min (see Pazzani & Rodonò 1981 and references therein), which might suggest that sympathetic flares also occur on stars. However, since most of the flare stars are members of binary systems, where the formation of gigantic magnetic loops interconnecting the two component stars has been suggested (Uchida & Sakurai 1983, Uchida 1986), magnetic reconnection at sites between the two stars' sites could lead to simultaneous flaring of both components. Nearly simultaneous events were observed on both components of BD +19 5116 AB (EQ Peg) using an optical area scanner (Rodonò 1978), and on AT Mic AB (Kundu et al 1987a) and UV Cet AB (Jackson et al 1987, Kundu et al 1987b) using the VLA.

## 8.4   Unconventional Flare Theories

The history of science is full of examples in which a marvelously constructed edifice of conventional wisdom has simply collapsed. As Kuhn's (1962) analysis of the scientific process suggested, the bulk of scientific research consists of adding little bits and pieces and decimal points to a preconceived paradigm, rather than boldly testing reality in every conceivable way. Nowadays we point with righteous ridicule at the Church prelates who refused to even look through Galileo's telescope as the epitome of unscientific obstinacy. In fact, wrong as they proved to be, their motives were hardly less well founded than our own: Aristotelan physics held that different physical laws than those on Earth governed the heavens; there was therefore no justification to take at face value the magnified sight of Jupiter's moons or Saturn's blurry ring produced by optics whose operation on celestial bodies followed unknown and probably different optical principles (Feyerabend 1975).

Letting the bandwagon rumble down main street as we step off to explore the back streets, we encounter several interesting theories. Ambartsumian (1954) formulated the concept that stellar flares arise from the dredging up of "protostellar material," and variations on this idea are being developed today for the Sun (see Tovmasyan & Zalinyan 1988). The solar neutrino rate has been claimed to correlate with sunspot number (Bahcall et al 1987); at an $^{37}Ar$ count rate $<1$ day$^{-1}$, time resolution is severely limited. Still, this is one piece of evidence used to infer that solar thermonuclear energy generation is variable and/or unstable, with thermonuclear flash-ups leading to creation of bubbles of some sort that travel from the core to the surface; these bubbles surface as shock fronts, resulting in explosions and creation of proton and electron beams via interaction with the magnetic field in the Convective Flare Theory of Grandpierre (1988). Following a different tack, Heristchi et al (1989) propose that low density plasmoids originate deep in the solar atmosphere and rise as a result of magnetic and buoyancy forces. These too explode at the surface. In this case, the chemical and isotopic composition and the energy spectra of flare particles in the interplanetary medium are invoked as issues better explained by the alternative flare theory.

The two-decade-old "fast electron hypothesis" begins with the assumption of a spontaneous appearance of almost monoenergetic electrons at $E \approx 1.5$ MeV (Gurzadyan 1988). If this happens, inverse Compton scattering of these rapidly moving electrons with the primarily infrared (in the case of dMe stars) photospheric radiation field will lead to production of more energetic photons (the $U$- and $B$-band flare), while at the same time decreasing the infrared flux above one micron; also, bremsstrahlung will

produce hard X rays. The infrared flux decrease in coincidence with intense optical flares, as reported by Rodonò & Cutispoto (1988) and Rodonò et al (1989), may also be interpreted in terms of increased H⁻ opacity owing to the ionization of metals during initial impulsive flare heatings (Grinin 1976, Henoux et al 1990a).

## 8.5  *Mystery Flares*

The appearance of an intense neutral potassium flare (7665 Å, 7699 Å) was reported for three stellar spectra at a certain well-known observatory in the early 1960s. The emission lines were real, but occurrence of the phenomenon was quite elusive. Sleuthing by Wing et al (1967) involved conducting a series of experiments in which the effect was reproduced ". . . if a match is struck at certain positions in the Coudé room during the exposure of an infrared spectrogram." One shudders to think of the cosmological ramifications of Hubble's ever-present pipe!

   The "potassium flare phenomenon" came to the attention of one of us (B.H.) because peculiar and unexplained emission lines did in fact manifest themselves one night in the spectrum of YZ CMi (Haisch & Giampapa 1985). These two lines at $\sim 4007$ Å and $\sim 4276$ Å remain unexplained to this day.[1]

## 9.   FOR THE FUTURE

Two lists of suggestions for future stellar research were recently included in the IAU Colloquium 104 on *Solar and Stellar Flares* and so will not be repeated here (Haisch 1989c, Foing 1989). We close with a brief discussion of a few more ideas.

## 9.1  *Solar Flare Prediction*

Operational solar flare predictions are made on the basis of active-region observation and classification, and empirical relationships between flare probability and active region class. For short-range (24 h) forecasts, this method has become reasonably reliable. However mid-range forecasts (up to 1 week) critically depend on prediction of the evolution of active regions.

---

[1] An amusing anecdote about academic writing style accompanied this incident. The revised and accepted manuscript concluded as follows: "We present these observations because they are intriguing and with the hope that a similar spectrum *may as a result be pulled out of a dusty drawer or may again manifest itself to a sleepy astronomer some dark and lonely night*." The author was naturally surprised to discover that the sentence appearing in the journal had been changed somewhere in press by the sober-minded editor (or his watchful assistant) to read: ". . . that a similar spectrum *sometime may be secured that exhibits similar properties*." Caveat author!

The development of an optimal classification scheme and statistics of evolutionary transitions from one class to another is now being actively pursued (e.g. Bornmann et al 1990; see also the report on "Bearalerts" by Zirin & Marquette 1990).

## 9.2   New Solar Flare Observations

Ever higher spatial and temporal resolution is an inevitable direction for pursuing flare processes. A moderately high-resolution HXR imaging experiment is being studied by NASA in the form of a joint large-space-structures and astrophysics experiment for the space shuttle called CASES (controls, astrophysics and structures experiment in space: a Fourier transform-type telescope on a long actively controlled boom). Ground-based multi-antenna radio interferometry at several simultaneous wavelengths is also undergoing rapid development (e.g. Gary & Hurford 1990).

As we achieve higher spatial and especially temporal resolution, we will soon begin to encounter situations in which the time scales of atomic processes (ionization, excitation, etc) dominate over the physical processes causing the changes (Golub et al 1989). This dominance will complicate analysis and interpretation even more primarily in the SXR line regime, which is one reason why one should look to the optical spectrum for new approaches, as for example in the analysis of Balmer and Na line spectra of Falchi et al (1990), or the correlation between hard X rays and chromospheric lines (Wei-Qun & Cheng 1990).

Henoux et al (1990a) have developed a somewhat detailed model of how a change in $H^-$ opacity resulting from particle beam ionization could result in a transient darkening on the Sun. They predict that such a "black light flare" should be observable at the same site and perhaps 20 s prior to the occurrence of a WLF. Negative contrasts of up to 15% are expected. The short duration and the typical proximity of such an occurrence to the penumbra make this phenomenon extremely difficult to catch.

The observation of "chromospheric condensation" downflows in chromospheric spectral lines could be a way of seeing the impulsive phase in stellar flares and deriving the time profile of the energy input (Fisher 1990).

Even in Hα, new investigations are possible. For example, Kitahara & Kurokawa (1990) identified impulsive brightenings using Hα photometry. Zirin & Tang (1990) review optical properties of impulsive flares and note that the largest solar flares show Hα broadening by up to 10 Å FWHM, which, if thermal, would imply temperatures of 1–4 MK in the middle chromosphere or lower.

## 9.3   Inter-Stellar Flares in RS CVn Systems

A standard type of loop analysis for two flares on the RS CVn binary II Peg results in loop lengths, $L \sim 6 \times 10^{10}$–$9 \times 10^{10}$ cm. In this system,

$R_* \approx 20 \times 10^{10}$ cm, and the binary separation is $a \approx 35 \times 10^{10}$ cm. Under these circumstances it makes sense to think of: loops extending high above the stellar surface, filaments located near the midpoint of the region between the stars, and even loops extending from one star to the other. The second of these possibilities has been explored by van den Oord (1988) as a means of storing the enormous magnetic energies released in such energetic RS CVn flares.

The rapidly rotating star AB Dor ($P = 0.514$ days; $v \sin i \approx 85$ km s$^{-1}$) appears to be a very young K0 dwarf in the final stages of evolving onto the main sequence. The quite long rise phases of two *Exosat* flares ($\sim 6000$ s) have been interpreted as evidence for loop structures with $L \sim$ few $\times R_*$ (Collier Cameron et al 1988).

In general, the exploration of the significant differences between the dMe and RS CVn flares should be an important area of investigation (Byrne 1989, see also Jeffries & Bedford 1990).

## 9.4   *Final Thoughts*

As we have seen, many lines of evidence point to a very small size scale, hence very high energy density, for the energization process of flares. For example, microwave bursts have been measured that are below the instrumental resolution of 20 ms, with radio brightness temperatures up to $10^{13}$ K (Gary et al 1990). It is possible that flare energy density may be much higher than we think at present and as a result even more exotic physics than MHD phenomena may be involved.

Taking the liberty of closing on a speculation, we suggest other physical processes that *may* turn out to be involved in flare energy release. There are strong arguments for fine scale currents on the Sun (see de Jager 1988, Parker 1989). Interesting observations and a theoretical model have been proposed (Ziolkowski & Tippett 1991) for the existence of a heretofore unrecognized current-carrying plasma state. Laboratory plasma discharge experiments indicate the existence of small-scale condensed charge systems in which electron densities may be on the order of $10^{20}$ to $10^{24}$ cm$^{-3}$ with negligible ion content. If such a plasma state occurs in the currents associated with solar flares, this could lead to interesting new processes of energy release and production of X rays. Following this speculation one step further, we note that in the presence of localized, extremely high electric fields, the vacuum state itself is thought to become unstable, allowing for the spontaneous creation of real particles (a phenomenon referred to as the "sparking of the vacuum"), thereby, in effect, deriving energy from the zero-point radiation field (Greenberg & Greiner 1982). The concept of a highly energetic vacuum is well established in modern physics; Misner et al 1973 state: ". . . the fluctuating electric field associated with (it) is among the most firmly established of physical effects."

Even though electromagnetic vacuum fluctuations produce the Lamb shift of spectral lines and a macroscopically measurable Casimir force, there continues to be lively debate over whether the field is real or virtual. Milonni (1988) presents a good discussion of vacuum-related phenomena, including the knotty relationship between the role of radiation reaction and vacuum field fluctuations in spontaneous emission. Astrophysical scenarios based on particle-vacuum interactions have recently been developed involving gravitation (Puthoff 1989), cosmic ray acceleration (Rueda 1990), etc. We speculate that it might prove to be fruitful to investigate a vacuum-related flaring mechanism.

Lastly, the role of quasi-static electric fields in the solar atmosphere has been generally passed over, but instead of launching into yet another review, we recommend the article by Foukal & Hinata (1991) and the textbook *Astrophysics of the Sun* by Foukal (1990).

*Literature Cited*

Aboudarham, J., Henoux, J. C. 1987. *Astron. Astrophys.* 174: 270
Aboudarham, J., Henoux, J. C. 1989. See Haisch & Rodonò 1989a, p. 19
Acton, L. W., Culhane, J. L., Gabriel, A. H. 1981. *Ap. J. Lett.* 254: L137
Acton, L. W., Canfield, R. C., Gunkler, T. A., Hudson, H. S., Kiplinger, A. L., Leibacher, J. W. 1982. *Ap. J.* 263: 409
Agrawal, P. C. 1988. *Astron. Astrophys.* 204: 235
Agrawal, P. C., Rao, A. R., Riegler, G. R. 1986. *MNRAS* 219: 777
Agrawal, P. C., Rao, A. R., Sreekantan, B. V. 1986. *MNRAS* 219: 225
Agrawal, P. C., Riegler, G. R., White, N. E. 1981. *MNRAS* 196: 73P

Alexander, D. 1990. *Astron. Astrophys.* 235: 431
Aly, J.-J., Kuijpers, J. 1990. Sterrekundig Inst. Utrecht preprint 89004
Ambartsumian, V. A. 1954. *Soobshch. Byurakan Obs.* 13: 3
Ambruster, C. W., Sciortino, S., Golub, L. 1987. *Ap. J. Suppl.* 65: 273
Andrews, A. D. 1989a. *Astron. Astrophys.* 210: 303
Andrews, A. D. 1989b. *Astron. Astrophys.* 214: 220
Andrews, A. D. 1990a. *Astron. Astrophys.* 229: 504
Andrews, A. D. 1990b. *Astron. Astrophys.* 227: 456
Andrews, A. D., Zembrowski, P. J., Hou-

debíne, E. R. 1990. *Astron. Astrophys.* In press

Aniol, R., Duerbeck, H. W., Seitter, W. C., Tsvetkov, M. K. 1990. In *Proc. IAU Symp.* 137

Antiochos, S. K. 1987. *Ap. J.* 312: 886

Antonucci, E. 1989. See Haisch & Rodonò 1989a, p. 31

Antonucci, E., Gabriel, A. H., Acton, L. W. 1982. *Sol. Phys.* 78: 107

Antonucci, E., Dodero, M. A., Martin, R. 1990. *Ap. J. Suppl.* 73: 137

Antonucci, E., Rosner, R., Tsinganos, K. 1986. *Ap. J.* 301: 975

Athay, R. G. 1984. *Sol. Phys.* 93: 123

Athay, R. G., Moreton, G. F. 1961. *Ap. J.* 133: 985

Bahcall, J. N., Field, G. B., Press, W. H. 1987. *Ap. J. Lett.* 320: L69

Bai, T. 1987. *Ap. J. Lett.* 318: L85

Bai, T. 1988. *Ap. J.* 334: 1049

Bai, T., Sturrock, P. A. 1989. *Annu. Rev. Astron. Astrophys.* 27: 421

Baliunas, S. L., Vaughan, A. H. 1985. *Annu. Rev. Astron. Astrophys.* 23: 379

Basri, G. S., Marcy, G. W. 1988. *Ap. J.* 330: 274

Bastian, T. S., Bookbinder, J., Dulk, G. A., Davis, M. 1990. *Ap. J.* 353: 265

Bastian, T. S., Bookbinder, J. A. 1987. *Nature* 326: 678

Bastian, T. S., Dulk, G. A., Slee, O. B. 1988. *Astron. J.* 95: 794

Belvedere, G., Paternò, L., Pidatella, R. M. 1989. *MNRAS* 237: 827

Bentley, R. D., Lemen, J. R., Phillips, K. J. H., Culhane, J. L. 1986. *Astron. Astrophys.* 154: 255

Benz, A. O. 1986. *Sol. Phys.* 104: 99

Benz, A. O., Simnett, G. M. 1986. *Nature* 320: 508

Beskin, G. M., Mitronova, S. N., Neizvestnyj, S. I., Plakhotnichenko, V. L., Pustil'nik, L. A., et al. 1989a. See Haisch & Rodonò 1989b, p. 95

Beskin, G. M., Plakhotnichenko, V. L., Pustil'nik, L. A., Shvartsman, V. F., Gershberg, R. E. 1989b. See Haisch & Rodonò 1989b, p. 99

Bogart, R. S., Bai, T. 1985. *Ap. J. Lett.* 299: L51

Boldt, E., Serlemitsos, P. 1969. *Ap. J.* 157: 557

Bopp, B. W. 1974. *MNRAS* 166: 79

Bornmann, P. L. 1987. *Ap. J.* 313: 449

Bornmann, P. L., Kalmbach, D., Kulhanek, D., Casale, A. 1990. Space Environ. Lab. Preprint

Bouwer, S. D. 1983. *J. Geophys. Res.* 10: 7823

Bromage, G. E., Phillips, K. J. H., Dufton, P. L., Kingston, A. E. 1986. *MNRAS* 220: 1021

Brown, J. C. 1971. *Sol. Phys.* 18: 489

Brown, J. C., Karlicky, M., MacKinnon, A. L., van den Oord, G. H. J. 1990. *Ap. J. Suppl.* 73: 343

Brown, W. A., Bruner, M. E., Acton, L. W., Mason, H. E. 1985. *Ap. J.* 301: 981

Brueckner, G. E., Bartoe, J.-D. F. 1983. *Ap. J.* 272: 329

Brueckner, G. E., Cook, J. W. 1990. *Ap. J.* 350: L21

Bruner, M. E., McWhirter, R. W. P. 1988. *Ap. J.* 326: 1002

Butler, C. J., Byrne, P. B., Andrews, A. D., Doyle, J. G. 1981. *MNRAS* 197: 215

Butler, C. J., Rodonò, M., Foing, B. H. 1988. *Astron. Astrophys.* 206: L1

Butler, C. J., Rodonò, M., Foing, B. H., Haisch, B. M. 1986. *Nature* 321: 679

Byrne, P. B. 1989. See Haisch & Rodonò 1989a, p. 61

Byrne, P. B., McKay, D. 1990. *Astron. Astrophys.* 227: 490

Byrne, P. B., Rodonò, M., eds. 1983. *Activity in Red-Dwarf Stars, IAU Coll. No. 71.* Dordrecht: Reidel

Canfield, R. C., Metcalf, T. R. 1987. *Ap. J.* 321: 586

Canfield, R. C., Zarro, D. M., Metcalf, T. R., Lemen, J. R. 1990. *Ap. J.* 348: 333

Carbonell, M., Ballester, J. L. 1990. *Astron. Astrophys.* 238: 377

Carmichael, H. 1964. In *AAS-NASA Symposium on the Physics of Solar Flares*, ed. W. N. Hess. NASA: SP-50, p. 451

Carrington, R. C. 1860. *MNRAS* XX: 13

Chen, J. 1989. *Ap. J.* 338: 453

Cheng, C.-C. 1990. *Ap. J.* 349: 362

Cheng, C.-C., Kjeldseth Moe, O. 1978. *Sol. Phys.* 59: 361

Cliver, E. W. 1983. *Sol. Phys.* 84: 347

Collier Cameron, A., Bedford, D. K., Rucinski, S. M., Vilhu, O., White, N. E. 1988. *MNRAS* 231: 131

Collura, A., Pasquini, L., Schmitt, J. H. M. M. 1988. *Astron. Astrophys.* 205: 197

Cristaldi, S., Rodonò, M. 1975. In *Variable Stars and Stellar Evolution, IAU Symp. 71.* Moscow: Ac. Publ., p. 75

Cristaldi, S., Gershberg, R. E., Rodonò, M. 1980. *Astron. Astrophys.* 89: 123

Datlowe, D. W., Elcan, M. J., Hudson, H. S. 1974. *Sol. Phys.* 39: 155

Datlowe, D. W., Hudson, H. S., Petterson, L. E. 1974. *Sol. Phys.* 35: 193

deJager, C. 1988. *Astrophys. Space Sci.* 144: 311

deJager, C., et al. 1986. *Astron. Astrophys.* 156: 95

deJager, C., et al. 1989. *Astron. Astrophys.* 211: 157

Dennis, B. R. 1985. *Sol. Phys.* 100: 465

Donati-Falchi, A., Falciani, R., Smaldone, L. A. 1985. *Astron. Astrophys.* 152: 165

Donnelly, R. F., Grubb, R. N., Cowley, F. C. 1977. *NOAA Tech. Mem.* ERL SEL-48

Doschek, G. A. 1990. *Ap. J. Suppl.* 73: 117
Doschek, G. A., Feldman, U. 1987. *Ap. J.* 313: 883
Doyle, J. G. 1989. *Astron. Astrophys.* 214: 258
Doyle, J. G., Butler, C. J. 1985. *Nature* 313: 378
Doyle, J. G., Byrne, P. B., van den Oord, G. H. J. 1989. *Astron. Astrophys.* 224: 153
Doyle, J. G., Mathioudakis, M. 1990. *Astron. Astrophys.* 227: 130
Drake, J. F. 1971. *Sol. Phys.* 16: 152
Dröge, W., Meyer, P., Evenson, P., Moses, D. 1989. See Haisch & Rodonò 1989a, p. 95
Dröge, W., Gibbs, K., Grunsfeld, J. M., et al. 1990. *Ap. J. Suppl.* 73: 279
Dulk, G. A. 1985. *Annu. Rev. Astron. Astrophys.* 23: 169
Dulk, G. A. 1987. In *Cool Stars, Stellar Systems and the Sun, Lecture Notes in Physics*, ed. J. L. Linsky, R. E. Stencel. Vol. 291, p. 72
Elwart, G. Z. 1961. *Z. Naturfors.* 9a: 637
Emslie, A. G. 1989. See Haisch & Rodonò, p. 105
Falchi, A., Falciani, R., Smaldone, L. A. 1990. *Ap. J. Suppl.* 84: 601
Falchi, A., Tozzi, G. P., Falciani, R., Smaldone, L. A. 1990. *Astron. Lett. Comm.* 28: 15
Feigelson, E. D., Giampapa, M. S., Vrba, F. J. 1990. In *The Sun in Time*, ed. C. P. Sonnett, M. S. Giampapa. Tucson: Univ. Ariz. Press
Feldman, U. 1990. *Ap. J.* 364: 322
Feldman, U., Doschek, G. A., Kreplin, R. W., Mariska, J. T. 1980. *Ap. J.* 241: 1175
Feyerabend, P. K. 1975. *Against Method.* Verso
Fisher, G. H. 1990. *Ap. J.* 346: 1019
Fisher, G. H., Hawley, S. L. 1990. *Ap. J.* 357: 243
Foing, B. H. 1989. See Haisch & Rodonò 1989a, p. 117
Forbes, T. G. 1990. *J. Geophys. Res.* 95: 11919
Foukal, P. 1990. *Astrophysics of the Sun.* Wiley-Interscience
Foukal, P., Hinata, S. 1991. *Sol. Phys.* 132: 307
Gabriel, A. H. 1972. *MNRAS* 160: 99
Gabriel, S., Evans, R., Feynman, J. 1990. *Sol. Phys.* 128: 415
Gary, D. E., Hurford, G., Flees, D. 1991. *Ap. J.* In press
Gary, D. E., Hurford, G. J. 1990. *Ap. J.* 361: 290
Gary, D. E., Linsky, J. L., Dulk, G. A. 1982. *Ap. J.* 263: L79
Gary, D. E., Moore, R. L., Hagyard, M. J., Haisch, B. M. 1987. *Ap. J.* 314: 782
Gershberg, R. E. 1989. *Mem. Soc. Astron. Ital.* 60: 263

Gershberg, R. E. 1967. *Astrofizika* 3: 127
Geyer, D. W., Harrington, R. S., Wurley, C. E. 1988. *Astron. J.* 95: 1841
Gibson, D. M. 1983. See Byrne & Rodonò 1983, p. 273
Giovanelli, R. G. 1948. *MNRAS* 108: 163
Gold, T., Hoyle, F. 1960. *MNRAS* 120: 89
Golub, L., Hartquist, T. W., Quillen, A. C. 1989. *Sol. Phys.* 122: 245
Gopalswamy, N., Kundu, M. R. 1987. *Sol. Phys.* 114: 347
Grandpierre, A. 1989. See Haisch & Rodonò 1989b, p. 365
Greenberg, J. S., Greiner, W. 1982. *Phys. Today*, August, p. 24
Greenstein, J. L. 1977. *Publ. Astron. Soc. Pac.* 89: 304
Grinin, V. P., Sobolev, V. V. 1988. *Astrofizica* 28: 355
Grinin, V. P., Sobolev, V. V. 1989. *Astrofizica* 31: 527
Grinin, V. P. 1976. *Izv. Krym. Astrofiz. Obs.* 55: 179
Grinin, V. P. 1983. See Byrne & Rodonò, p. 613
Gurzadyan, G. A. 1988. *Ap. J.* 332: 183
Hagyard, M. J. 1988. *Sol. Phys.* 115: 107
Hagyard, M. J. 1990. MSFC SSL Preprint 90–104
Hagyard, M. J., Low, B. C., Tandberg-Hanssen, E. 1981. *Sol. Phys.* 80: 33
Hagyard, M. J., Moore, R. L., Emslie, A. G. 1984. *Adv. Sp. Res.* 4(7), 71
Haisch, B. M. 1986. *Ir. Astron. J.* 17: 200
Haisch, B. M. 1989a. In *Magill's Survey of Science: Space Expl. Series*, ed. F. M. Magill, p. 1315. Pasadena: Salem
Haisch, B. M. 1989b. *Astron. Astrophys.* 219: 317
Haisch, B. M. 1989c. See Haisch & Rodonò 1989a, p. 121
Haisch, B. M., Butler, C. J., Doyle, J. G., Rodonò, M. 1987. *Astron. Astrophys.* 181: 96
Haisch, B. M., Butler, C. J., Foing, B., Rodonò, M., Giampapa, M. S. 1990b. *Astron. Astrophys.* 230: 419
Haisch, B. M., Giampapa, M. S. 1985. *Publ. Astron. Soc. Pac.* 97: 340
Haisch, B. M., Linsky, J. L., Bornmann, P. L., Stencel, R. E., Antiochos, S. K., Golub, L., Vaianai, G. S. 1983. *Ap. J.* 267: 280
Haisch, B. M., Linsky, J. L., Lampton, M., Paresce, F., Margon, B., Stern, R. 1977. *Ap. J. Lett.* 213: L119
Haisch, B. M., Rodonò, M., eds. 1989a. *Solar and Stellar Flares, IAU Coll. 104.* Dordrecht: Kluwer
Haisch, B. M., Rodonò, M., eds. 1989b. *Solar and Stellar Flares, Poster Papers, IAU Coll. 104*, Publ. Catania Astrophys. Obs., Special Volume

Haisch, B. M., Schmitt, J. H. M. M., Rodonò, M., Gibson, D. M. 1990a. *Astron. Astrophys.* 232: 387

Haisch, B. M., Simon, T. 1982. *Ap. J.* 263: 252

Haisch, B. M., Strong, K. T., Harrison, R. A., Gary, G. A. 1988. *Ap. J. Suppl.* 68: 371

Harrison, R. A., Hildner, E., Hundhausen, A. J., Sime, D. G., Simnett, G. M. 1990. *J. Geophys. Res.* 95: 917

Harrison, R. A., Pearce, G., Skumanich, A. 1988. *Ap. J.* 332: 1058

Harrison, R. A., Sime, D. G. 1989. *Astron. Astrophys.* 208: 274

Hartmann, L. 1987. *Lecture Notes in Physics* 291: 1

Heise, J., Brinkman, A. C., Schriguer, J. 1975. *Ap. J. Lett.* 202: L73

Henoux, J.-C., Aboudarham, J., Brown, J. C., van den Oord, G. H. J., van Driel-Gesztelyi, L., Gerlie, O. 1990a. *Astron. Astrophys.* 233: 577

Henoux, J. C., Chambe, G., Smith, D., et al. 1990b. *Ap. J. Suppl.* 73: 303

Heristchi, D. 1986. *Ap. J.* 311: 474

Heristchi, D., Raadu, M. A., Vial, J.-C., Malherbe, J.-M. 1989. See Haisch & Rodonò 1989b, p. 321

Heyvaerts, J. 1981. In *Solar Flare Magnetohydrodynamics*, ed. E. R. Priest, p. 429. New York: Gordon & Breach

Hiei, E. 1982. *Sol. Phys.* 80: 113

Hiei, E. 1987. *Sol. Phys.* 113: 249

Hirayama, T. 1974. *Sol. Phys.* 34: 323

Hjellming, R. M., Gibson, D. M. 1980. In *Radio Physics of the Sun*, ed. M. R. Kundu, T. E. Gergely, p. 209. Dordrecht: Reidel

Hodgson, R. 1860. *MNRAS* XX: 15

Holman, G. D. 1985. *Ap. J.* 293: 584

Holman, G. D. 1987. In *Lecture Notes in Physics*, ed. M. Zeilik, D. Gibson, 254: 271

Houdebine, E. R., Butler, C. J., Panagi, P. M., Rodonò, M., Foing, B. H. 1991. *Astron. Astrophys. Suppl.* 87: 33

Houdebine, E. R., Foing, B. H. 1991. *Astron. Astrophys.* Submitted

Houdebine, E. R., Rodonò, M., Foing, B. H. 1990. *Astron. Astrophys.* 238: 249

Hudson, H. S. 1972. *Sol. Phys.* 24: 414

Hudson, H. S. 1987. *Sol. Phys.* 113: 1

Hudson, H. S. 1991. *Sol. Phys.* In press

Ichimoto, I., Kubota, J., Suzuki, M., Tohmura, I., Kurookawa, H. 1985. *Nature* 316: 422

Ionson, J. A. 1982. *Ap. J.* 254: 318

Jackson, P. D., Kundu, M. R., White, S. M. 1987. *Ap. J.* 316: L85

Jackson, P. D., Kundu, M. R., White, S. M. 1989. *Astron. Astrophys.* 210: 284

Jeffries, R. D., Bedford, D. K. 1990. *MNRAS* 246: 337

Joy, A. H., Humason, M. L. 1949. *Publ. Astron. Soc. Pac.* 133

Kaastra, J. S. 1985. *Solar Flares: An Electrodynamic Model.* Thesis, Univ. of Utrecht

Kane, S. R., Fenimor, E. E., Klebesadel, R. W., Laros, J. G. 1988. *Ap. J.* 326: 1017

Kane, S. R., Love, J. J., Neidig, D. F., Cliver, E. W. 1985. *Ap. J.* 290: L45

Kappenman, J. G., Albertson, V. D. 1990. *IEEE Spectrum*, March: 27

Katsova, M. M., Livshits, M. A. 1987. In *Activity in Cool Star Envelopes, Tromso, 1–8 July 1987*

Kiepenheuer, K. O. 1964. In *AAS-NASA Symposium on the Physics of Solar Flares*, ed. W. N. Hess. NASA: SP-50, p.323

Kitahara, T., Kurokawa, H. 1990. *Sol. Phys.* 125: 321

Klimchuk, J. A., Sturrock, P. A. 1989. *Ap. J.* 345: 1034

Kocharov, G. E. 1987. *Sov. Sci. Rev. Astrophys. Space Phys.* 6: 155

Kopp, R. A., Poletto, G. 1984. *Sol. Phys.* 93: 351

Kuhn, T. S. 1962. The Structure of Scientific Revolutions

Kuijpers, J. 1989. See Haisch & Rodonò 1989a, p. 163

Kundu, M. R., Jackson, P. D., White, S. M., Melozzi, M. 1987a. *Ap. J.* 312: 822

Kundu, M. R., Jackson, P. D., White, S. M. 1987b. *Fifth Cambridge Workshop on Cool Stars*, p. 100. Berlin: Springer

Kundu, M. R., Lang, K. R. 1985. *Science* 228: 9

Kundu, M. R., Pallavicini, R., White, S. M., Jackson, P. D. 1988. *Astron. Astrophys.* 195: 159

Kunkel, W. E. 1975. In *Variable Stars and Stellar Evolution*, ed. V. E. Sherwood, L. Plant, p. 15. Dordrecht: Reidel

Landini, M., Monsignori-Fossi, B. C. 1990. *Astron. Astrophys. Suppl.* 82: 229

Landini, M., Monsignori-Fossi, B. C., Pallavicini, R., Piro, L. 1986. *Astron. Astrophys.* 157: 217

Lang, K. R. 1990. In *Flare Stars in Star Clusters, Associations and Solar Vicinity, IAU Symp. 137*, ed. L. V. Mirzoyan. Dordrecht: Kluwer

Lang, K. R., Bookbinder, J. A., Golub, L., Davis, M. M. 1983. *Ap. J. Lett.* 272: L15

Lang, K. R., Willson, R. F. 1986. *Ap. J. Lett.* 302: L17

Lang, K. R., Willson, R. F. 1988. *Ap. J.* 326: 300

LaRosa, T. N. 1990. *Sol. Phys.* 126: 153

Lean, J. L., Brueckner, G. E. 1989. *Ap. J.* 337: 568

Li, P., Emslie, G. 1990. *Sol. Phys.* 129: 113

Lin, R. P., Schwartz, R. A., Kane, S. R., et al. 1984. *Ap. J.* 283: 421

Lin, R. P., Hudson, H. S. 1971. *Sol. Phys.* 17: 412

Lin, R. P., Schwartz, R. A., Pelling, R. M., Hurley, K. C. 1981. *Ap. J. Lett.* 251: L109

Linford, G. A., Lemen, J. R., Strong, K. T. 1988. *Adv. Space Res.* 8: 11

Linford, G. A., Wolfson, C. J. 1989. *Ap. J.* 331: 1036

Linsky, J. L., Neff, J. E., Brown, A., et al. 1989. *Astron. Astrophys.* 211: 173

Linsky, J. L. 1989. See Haisch & Rodonò 1989a, p. 187

Livi, S. H. B., Martin, S., Wang, H., Ai, G. 1989. See Haisch & Rodonò 1989a, p. 197

Lovell, B., Whipple, F. L., Solomon, L. H. 1963. *Nature* 198: 228

Lovell, B., Whipple, F. L., Solomon, L. H. 1964. *Nature* 202: 377

Low, B. D. 1977. *Ap. J.* 212: 234

Lu, E. T., Petrosian, V. 1990. *Ap. J.* 354: 735

Mauas, P. J. D. 1990. *Ap. J. Suppl.* 74: 609

MacKinnon, A. L. 1989. *Astron. Astrophys.* 226: 284

Machado, M. E., Emslie, A. G., Avrett, E. H. 1989. *Sol. Phys.* 124: 303

Martens, P. C. H. 1988. *Ap. J. Lett.* 330: L131

Martens, P. C. H., Kuin, N. P. M. 1989. *Sol. Phys.* 122: 263

Martens, P. C. H., Young, A. 1990. *Ap. J. Suppl.* 73: 333

Martin, S. F. 1990. In *Lecture Notes in Physics No. 363: Dynamics of Quiescent Prominences*, ed. V. Ruzdjak, E. Tandburg-Hanssen, p. 1. New York: Springer-Verlag

Mathioudakis, M., Doyle, J. G. 1990. *Astron. Astrophys.* 232: 114

Mayfield, E. B., Lawrence, J. K. 1985. *Sol. Phys.* 96: 293

McClements, K. G. 1987. *Sol. Phys.* 109: 355

McClements, K. G. 1989. *Astron. Astrophys.* 208: 279

McWhirter, R. W. P., Thonemann, P. C., Wilson, R. 1975. *Astron. Astrophys.* 40: 63

Melrose, D. B., Dulk, G. A. 1987. *Physica Scripta* T18: 29

Metcalf, T. R., Canfield, R. C., Avrett, E. H., Metcalf, F. T. 1990. *Ap. J.* 350: 463

Mewe, R., Gronenschild, E. H. B. M., van den Oord, G. H. J. 1985. *Astron. Astrophys. Suppl.* 62: 197

Meyer, J.-P. 1985a. *Ap. J. Suppl.* 57: 151

Meyer, J.-P. 1985b. *Ap. J. Suppl.* 57: 173

Mirzoyan, L. V., Ambaryan, V. V., Garibdzhanyan, A. T., Mirzoyan, A. L. 1988. *Astrofizica* 29: 531

Misner, C. W., Thorne, K. S., Wheeler, J. A. 1973. *Gravitation*. San Francisco: Freeman

Moffett, T. J. 1972. *Nature Phys. Sci.* 240: 41

Moffett, T. J. 1974. *Ap. J. Suppl.* 29: 1

Montmerle, T. 1984. *Proc. XXV COSPAR*

Montmerle, T. 1990. In *Proc. of Star Formation and Early Stellar Evolution*, ed. N. Kylafis, C. J. Lada. Preprint

Moore, R. L. 1988. *Ap. J.* 324: 1132

Moreton, G. E., Ramsey, H. E. 1960. *Publ. Astron. Soc. Pac.* 72: 356

Moses, D., Dröge, W., Meyer, P., Evenson, P. 1989. *Ap. J.* 346: 523

Mullan, D. J. 1976. *Ap. J.* 104: 530

Mullan, D. J. 1984. *Ap. J.* 282: 603

Munro, R. H., Gosling, J. T., Hildner, E., MacQueen, R. M., Poland, A. I., Ross, C. L. 1979. *Sol. Phys.* 61: 201

Neidig, D. F. 1989. See Haisch & Rodonò 1989a, p. 261

Neidig, D. F., Wiborg, P. H., Gilliam, L. B. 1989. *NSO Tech. Rept. 89-001*

Neupert, W. M. 1989. *Ap. J.* 344: 504

Nitta, N., Kosugi, T. 1986. *Sol. Phys.* 105: 73

Orrall, F. Q., ed. 1981. *Solar Active Regions*. Boulder: Colo. Assoc. Univ. Press

Orrall, F. Q., Zirker, J. B. 1976. *Ap. J.* 208: 618

Pallavicini, R., Golub, L., Rosner, R., Vaiana, G. S. 1982. *SAO Spec. Rept.* 392: 77

Pallavicini, R., Monsignori-Fossi, B. C., Landini, M., Schmitt, J. H. M. M. 1988. *Astron. Astrophys.* 191: 109

Pallavicini, R., Serio, S., Vaiana, G. S. 1977. *Ap. J.* 216: 108

Pallavicini, R., Tagliaferri, G., Pollock, A. M. T., Schmitt, J. H. M. M., Rosso, C. 1990a. *Astron. Astrophys.* 227: 483

Pallavicini, R., Tagliaferri, G., Stella, L. 1990b. *Astron. Astrophys.* 228: 403

Parker, E. N. 1987. *Sol. Phys.* 111: 297

Parker, E. N. 1988. *Ap. J.* 330: 474

Parker, E. N. 1989. See Haisch & Rodonò 1989a, p. 271

Pazzani, V., Rodonò, M. 1981. *Astrophys. Space Sci.* 27: 347

Pearce, G., Harrison, R. A. 1988. *Astron. Astrophys.* 206: 121

Pearce, G., Harrison, R. A. 1990. *Astron. Astrophys.* 228: 513

Pearson, D. H., Nelson, R., Kajoian, G., Seal, J. 1989. *Ap. J.* 336: 1050

Perez-Peraza, J. 1986. *Space Sci. Rev.* 44: 91

Peter, Th., Ragoozin, E. N., Urnov, A. M., Uskov, D. B., Rust, D. M. 1990. *Ap. J.* 351: 317

Pettersen, B. R. 1976. *Catalogue of Flare Stars, Rept. No. 46.* Oslo

Pettersen, B. R. 1989. See Haisch & Rodonò 1989a, p. 299

Pick, M., Klein, K.-L., Trottet, G. 1990. *Ap. J. Suppl.* 73: 165

Pneuman, G. W. 1980. In *Solar and Interplanetary Dynamics, IAU Symp. 91*, ed. M. Dryer, E. Tandberg-Hanssen, p. 317

Pneuman, G. W. 1984. *Sol. Phys.* 94: 387

Poletto, G. 1989. See Haisch & Rodonò 1989a, p. 313

Poletto, G., Pallavicini, R., Kopp, R. A. 1988. *Astron. Astrophys.* 201: 93

Porter, J. G., Moore, R. L., Reichmann, E. J., Engvold, O., Harvey, K. L. 1987. *Ap. J.* 323: 380

Porter, J. G., Toomre, J., Gebbie, K. B. 1984. *Ap. J.* 283: 879

Priest, E. R. 1982. *Solar Magneto-Hydro-dynamics.* Dordrecht: Reidel

Priest, E. R. 1988. *Ap. J.* 328: 848

Puthoff, H. E. 1989. *Phys. Rev. A* 39: 2333

Pye, J. P., McHardy, I. M. 1983. *MNRAS* 205: 875

Ramaty, R., Murphy, R. J. 1987. *Space Sci. Rev.* 45: 213

Raoult, A., Pick, M., Dennis, B. R., Kane, S. R. 1985. *Ap. J.* 299: 1027

Raymond, J. C. 1990. *Ap. J.* 365: 387

Raymond, J. C., Cox, D. P., Smith, B. W. 1976. *Ap. J.* 204: 290

Reale, F., Peres, G., Serio, S., Rosner, R., Schmitt, J. H. M. M. 1988. *Ap. J.* 328: 256

Reames, D. V. 1990. *Ap. J. Suppl.* 73: 235

Rieger, E., Share, G. H., Forrest, D. J., et al. 1984. *Nature* 312: 623

Robinson, R. D. 1980. *Ap. J.* 239: 961

Robinson, R. D., Worden, S. P., Harvey, J. W. 1980. *Ap. J. Lett.* 236: L155

Rodonò, M. 1974. *Astron. Astrophys.* 32: 337

Rodonò, M. 1978. *Astron. Astrophys.* 66: 175

Rodonò, M., Pucillo, M., Sedmak, G., De Biase, G. A. 1979. *Astron. Astrophys.* 76: 242

Rodonò, M., Cutispoto, G., Linsky, J. L., et al. 1984. *Proc. Fourth Eur. IUE Conf.* ESA SP-218, p. 247

Rodonò, M., Houdebine, E. R., Catalano, S., et al. 1989. See Haisch & Rodonò 1989b, p. 53

Rodonò, M. 1986a. In *Flare Stars and Related Objects*, ed. L. V. Mirzoyan, p. 19. Erevan: Publ. Armenian Ac. Sci.

Rodonò, M. 1986b. *The M-Type Stars*, ed. H. R. Johnson, F. Querci, CNRS-NASA Monograph Ser. on Nonthermal Pheno-mena in Stellar Atmospheres, NASA SP-492, p. 409

Rodonò, M., Cutispoto, G. 1988. In *Activity in Cool Star Envelopes*, ed. O. Havnes, et al., p. 163. Dordrecht: Kluwer

Rutten, R. G. M., Schrijver, C. J., Zwaan, C., Duncan, D. K., Mewe, R. 1989. *Astron. Astrophys.* 219: 239

Saar, S. H. 1987. In *Fifth Cambridge Work-shop on Cool Stars, Stellar Systems, and the Sun*, ed. J. L. Linsky, M. R. Stencel, p. 10. Berlin: Springer

Saar, S. H. 1988. *Ap. J.* 324: 441

Saar, S. H., Huovelin, J., Giampapa, M., Linsky, J. L., Jordan, C. 1988. In *Cool Star Envelopes*, ed. O. Havnes, et al., p. 45. Dordrecht: Kluwer

Saar, S. H., Linsky, J. L. 1985. *Ap. J.* 299: L47

Saar, S. H., Linsky, J. L., Beckers, J. M. 1986. *Ap. J.* 302: 777

Saba, J., Strong, K. T. 1990. *Ap. J.* Sub-mitted

Sakai, J.-I. 1990. *Ap. J. Suppl.* 73: 321

Sawyer, C., Warwick, J. W., Dennett, J. T. 1986. *Solar Flare Prediction.* Boulder: Colo. Assoc. Univ. Press

Schaeffer, B. E. 1989. *Ap. J.* 337: 927

Schmitt, J. H. M. M., Rosso, C. 1988. *Astron. Astrophys.* 191: 99

Severny, A. B. 1958. *Isz. Krym. Astrofiz. Obs.* 1: 102

Shakhovskaya, N. I. 1989. See Haisch & Rodonò 1989a, p. 375

Shibata, K., Tajima, T., Matsumoto, R., et al. 1989. *Ap. J.* 338: 471

Simnett, G. M. 1986. *Sol. Phys.* 106: 165

Simnett, G. M., Haines, M. G. 1990. *Proc. XXI Intl. Cosmic Ray Conference, Adel-aide*

Simnett, G. M., Mouradian, Z., Martres, M.-J., Soru-Escaut, I. 1989. *Astron. Astro-phys.* 224: 284

Simnett, G. M., Strong, K. T. 1984. *Ap. J.* 284: 839

Skumanich, A. 1985. *Aust. J. Phys.* 38: 971

Skumanich, A. 1986. *Ap. J.* 309: 858

Slee, O. B., Solomon, L. H., Patson, G. E. 1963. *Nature* 199: 991

Smith, H. J., Smith, E. v. P. 1963. *Solar Flares*

Spangler, R. S., Moffett, T. J. 1976. *Ap. J.* 203: 497

Stern, R. A., Underwood, J. H., Antiochos, S. K. 1983. *Ap. J.* 264: L55

Stern, R. A., Haisch, B. M., Nagase, F., Uchida, Y., Tsuneta, S. 1990a. In *Astron. Soc. Pac. Conf. Series* 9: 224

Stern, R. A., Haisch, B. M., Uchida, Y., et al. 1990b. In *Astron. Soc. Pac. Conf. Series* 9: 227

Strong, K. T., Benz, A. O., Dennis, B. R., et al. 1984. *Sol. Phys.* 91: 325

Strong, K. T., Lemen, J. R., Linford, G. A. 1990. *Adv. Space Res.* In press

Sturrock, P. A. 1980. *Solar Flares: A Mono-graph from Skylab Solar Workshop II*

Sturrock, P. A. 1987. *Sol. Phys.* 113: 13

Sturrock, P. A., Dixon, W. W., Klimchuk, J. A., Antiochos, S. K. 1990. *Ap. J.* 356: L31

Sturrock, P. A., Kaufman, P., Moore, R. L., Smith, D. F. 1984. *Sol. Phys.* 94: 341

Sturrock, P. A., Stern, R. A. 1980. *Ap. J.* 238: 98

Sturrock, P. A., Uchida, Y. 1981. *Ap. J.* 246: 331

Svestka, Z. 1976. *Solar Flares.* Dordrecht: Reidel

Svestka, Z. 1987. *Sol. Phys.* 108: 411

Svestka, Z. 1989. See Haisch & Rodonò 1989a, p. 389

Swank, J. H., Johnson, H. M. 1982. *Ap. J. Lett.* 259: L67

Swank, J. H., White, N. E., Holt, S. S., Becker, R. H. 1981. *Ap. J.* 246: 208

Sylwester, J., Lemen, J. R., Mewe, R. 1984. *Nature* 310: 665

Szécsényi-Nagy, G. 1990. *Astrophys. Space Sci.* 170: 63

Tagliaferri, G., Doyle, J. G., Giommi, P. 1990. *Astron. Astrophys.* 231: 131

Tanaka, K. 1983. See Byrne & Rodonò 1983, p. 307

Tanaka, K. 1986. *Publ. Astron. Soc. Jpn.* 38: 225

Tanaka, K. 1987. *Publ. Astron. Soc. Jpn.* 39: 1

Tandberg-Hanssen, E., Emslie, A. G. 1988. *The Physics of Solar Flares.* Cambridge: Cambridge Univ. Press

Thomas, R. J., Starr, R., Crannell, C. J. 1985. *Sol. Phys.* 95: 323

Thomas, R. J., Teske, R. G. 1971. *Sol. Phys.* 16: 431

Tsuneta, S. 1983. *ISAS Report No. 239*

Tsvetkov, M. K., Tsvetkova, K. P. 1990. In *Proc. IAU Symp. 137*

Tovmasyan, G. M., Zalinyan, V. P. 1988. *Astrofizica* 28: 131

Uchida, Y. 1986. In *Highlights of Astronomy*, ed. J. P. Swings, p. 461. Dordrecht: Reidel

Uchida, Y., Sakurai, T. 1983. See Byrne & Rodonò 1983, p. 629

Uralov, A. M. 1990. *Sol. Phys.* 127: 253

Vaiana, G. S., Kreiger, A. S., Timothy, A. F. 1973. *Sol. Phys.* 32: 81

van Ballegooijen, A. A., Martens, P. C. H. 1989. *Ap. J.* 343: 971

van den Oord, G. H. J. 1988. *Astron. Astrophys.* 205: 167

van den Oord, G. H. J., Mewe, R. 1989. *Astron. Astrophys.* 213: 245

van den Oord, G. H. J., Mewe, R., Brinkman, A. C. 1988. *Astron. Astrophys.* 205: 181

Van Speybroek, L. P., Krieger, A. S., Vaiana, G. S. 1970. *Nature* 227: 818

Van Tend, W., Kuperus, M. 1978. *Sol. Phys.* 59: 115

Vestrand, W. T., Forrest, D. J., Chupp, E. L., Rieger, E., Share, G. H., et al. 1987. *Ap. J.* 322: 1010

Vilhu, O., Ambruster, C. W., Neff, J. E., et al. 1989. *Astron. Astrophys.* 222: 179

Vrsnak, B., Ruzdjak, V., Messerotti, M., Zlobec, P. 1987. *Sol. Phys.* 111: 23

Watanabe, T. 1987. *Sol. Phys.* 113: 107

Webb, D. F., Hundhausen, A. J. 1987. *Sol. Phys.* 108: 383

Wie-Qun, G., Cheng, F. 1990. *Sol. Phys.* 125: 333

Whitehouse, D. R. 1985. *Astron. Astrophys.* 145: 449

Widing, K. G., Feldman, U. 1989. *Ap. J.* 344: 1046

Wild, J. P. 1950a. *Aust. J. Sci.* A3: 387

Wild, J. P. 1950b. *Aust. J. Sci.* A3: 531

Wing, R. F., Peimbert, M., Spinrad, H. 1967. *Publ. Astron. Soc. Pac.* 79: 351

Winglee, R. M., Dulk, G. A. 1986. *Ap. J.* 307: 808

Wolfson, C. J., Doyle, J. G., Leibacher, J. W., Phillips, K. J. H. 1984. *Ap. J.* 289: 319

Worden, S. P., Peterson, B. M. 1976. *Ap. J. Lett.* 206: L145

Worden, S. P., Schneeberger, T. J., Giampapa, M. S. 1981. *Ap. J. Suppl.* 46: 159

Zappalà, R. A., Zuccarello, F. 1989. *Astron. Astrophys.* 214: 369

Zarro, D. M., Canfield, R. C., Strong, K. T., Metcalf, T. R. 1988. *Ap. J.* 324: 582

Zirin, H. 1988. *Solar Astrophysics.* Cambridge: Cambridge Univ. Press

Zirin, H., Marquette, W. 1990. *Solar Phys.* In press

Zirin, H., Tang, F. 1990. *Ap. J. Suppl.* 73: 111

Ziolkowski, R. W., Tippett, M. K. 1991. *Phys. Rev. A* 43: 3066

ADDED IN PROOF

Boyer, T. H. 1975. *Phys. Rev. D* 11: 790

Milonni, P. W. 1988. *Phys. Scr.* T21: 102

Najita, K., Orrall, F. Q. 1970. *Sol. Phys.* 15: 176

Rueda, A. 1990. *Space Sci. Rev.* 53: 223